Full dimensional Franck-Condon factors for the acetylene [~ over A] [superscript 1]A[subscript u] — [~ over X] [superscript 1#[+ over g] transition. I. Method for calculating polyatomic linear—bent vibrational intensity factors and evaluation of calculated intensities for the gerade vibrational modes in acetylene

Citation: Park, G. Barratt. "Full Dimensional Franck-Condon Factors for the Acetylene [~ over A] [superscript 1]A[subscript u] — [~ over X] [superscript 1Σ[+ over g] Transition. I. Method for Calculating Polyatomic Linear—bent Vibrational Intensity Factors and Evaluation of Calculated Intensities for the Gerade Vibrational Modes in Acetylene." The Journal of Chemical Physics 141, no. 13 (October 7, 2014): 134304. © 2014 AIP Publishing LLC

As Published: http://dx.doi.org/10.1063/1.4896532

Publisher: American Institute of Physics (AIP)

Persistent URL: http://hdl.handle.net/1721.1/96882

Version: Final published version: final published article, as it appeared in a journal, conference proceedings, or other formally published context

Full dimensional Franck-Condon factors for the acetylene $\tilde{A}\ ^1A_u$—$\tilde{X}\ ^1\Sigma_g^+$ transition. I. Method for calculating polyatomic linear—bent vibrational intensity factors and evaluation of calculated intensities for the *gerade* vibrational modes in acetylene

G. Barratt Park[a)]
Department of Chemistry, Massachusetts Institute of Technology, Cambridge, Massachusetts 02139, USA

(Received 12 May 2014; accepted 26 August 2014; published online 3 October 2014)

Franck-Condon vibrational overlap integrals for the $\tilde{A}\ ^1A_u$—$\tilde{X}\ ^1\Sigma_g^+$ transition in acetylene have been calculated in full dimension in the harmonic normal mode basis. The calculation uses the method of generating functions first developed for polyatomic Franck-Condon factors by Sharp and Rosenstock [J. Chem. Phys. **41**(11), 3453–3463 (1964)], and previously applied to acetylene by Watson [J. Mol. Spectrosc. **207**(2), 276–284 (2001)] in a reduced-dimension calculation. Because the transition involves a large change in the equilibrium geometry of the electronic states, two different types of corrections to the coordinate transformation are considered to first order: corrections for axis-switching between the Cartesian molecular frames and corrections for the curvilinear nature of the normal modes at large amplitude. The angular factor in the wavefunction for the out-of-plane component of the trans bending mode, ν_4'', is treated as a rotation, which results in an Eckart constraint on the polar coordinates of the bending modes. To simplify the calculation, the other degenerate bending mode, ν_5'', is integrated in the Cartesian basis and later transformed to the constrained polar coordinate basis, restoring the conventional v and l quantum numbers. An updated $\tilde{A}$-state harmonic force field obtained recently in the R. W. Field research group is evaluated. The results for transitions involving the *gerade* vibrational modes are in qualitative agreement with experiment. Calculated results for transitions involving *ungerade* modes are presented in Paper II of this series [G. B. Park, J. H. Baraban, and R. W. Field, "Full dimensional Franck–Condon factors for the acetylene $\tilde{A}\ ^1A_u$—$\tilde{X}\ ^1\Sigma_g^+$ transition. II. Vibrational overlap factors for levels involving excitation in *ungerade* modes," J. Chem. Phys. **141**, 134305 (2014)]. © *2014 AIP Publishing LLC*. [http://dx.doi.org/10.1063/1.4896532]

I. INTRODUCTION

The $\tilde{A}\ ^1A_u(C_{2h})$—$\tilde{X}^1\Sigma_g^+(D_{\infty h})$ transition in acetylene has been the subject of extensive spectroscopic and theoretical investigation. In the 1950s, Ingold and King[1,2]—and later Innes[3]—performed the first detailed analysis of the band structure. They showed that a linear to trans-bent geometry change takes place upon excitation from the $D_{\infty h}$ ground state to the C_{2h} excited state. Acetylene was the first molecular system in which a qualitative change in geometry and symmetry accompanying an electronic excitation was proven by spectroscopic methods. Since that time, both the $\tilde{X}$ and $\tilde{A}$ states of acetylene have been spectroscopically characterized in great detail.[4–37]

In spite of the wealth of data available, it has been challenging to make quantitative predictions for $\tilde{A}$—$\tilde{X}$ spectral intensities. Although the Franck-Condon principle has long guided the interpretation of vibrational intensity factors, the calculation of FC factors for polyatomic molecules remains challenging—especially in cases where there is a large change in equilibrium geometry and a qualitative change in symmetry between the states in question. The multidimensional nature of the polyatomic vibrational problem not only introduces interactions between the degrees of freedom on each potential energy surface, but it also complicates the transformation between the coordinates of the two states. So, in addition to the shift of origin and frequency scaling that are familiar from diatomic molecules, polyatomic molecules also exhibit Duschinsky rotation,[38] as a result of the non-diagonal (and in general nonlinear) transformation between the normal mode coordinates. Furthermore, for transitions involving a change from linear to bent reference configurations, there is an inherent interplay between vibrational and rotational degrees of freedom, because vibrational angular momentum of the linear state correlates with rotation in the bent state, and the number of vibrational degrees of freedom typically used to describe the linear and bent configurations is different.

Due to the importance of FC factors in polyatomic molecules, numerous approaches have been taken by various authors. Reference 39 provides a list of citations. There is no consensus on the best general formulation of the problem and most authors have tailored their methods to the molecular transition at hand. The most common approaches involve variations on the method introduced by Sharp and Rosenstock,[40] which involves direct integration of harmonic wavefunctions obtained by the method of generating functions.

a)Electronic mail: barratt@mit.edu

Relatively little attention has been paid to the calculation of FC factors for systems involving linear to bent geometry changes. Smith and Warsop[41] pointed out the need for inclusion of rotational coordinates in linear to bent transitions, but they did not address the problem further. Kovner *et al.*[42] calculated Franck-Condon factors for the $^1B_2 \rightarrow {}^1\Sigma_g^+$ transition in CO_2 in full dimension. For the degenerate bending mode of the linear molecule, these authors use degenerate bending wavefuctions, which are separable into a radial factor (a generalized Laguerre polynomial that depends on v, l, and the radial coordinate ρ) and an angular factor (depending on l and the polar angle ϕ). They include the radial factor in the vibrational integral, but they treat the angular factor as part of the rotational integral, and they successfully calculate rovibrational intensity factors by approximating the bent state as a symmetric top. The research groups of Vaccaro co-workers have successfully applied methods, based on Lie algebra formalisms,[43] to the bent-linear transition in HCP.[44]

After the pioneering works of Ingold, King, and Innes, several authors considered the one-dimensional Franck-Condon factors for the trans-bending progression of the acetylene $\tilde{A}$—$\tilde{X}$ transition.[2,41,45] More recently, Watson has calculated reduced-dimension Franck-Condon overlaps for the three *gerade* vibrational modes by extending the method of Sharp and Rosenstock[40] to treat a linear-to-bent transition, including axis-switching effects.[46] Watson's treatment of the vibrational and rotational degrees of freedom are analogous to those used by Kovner *et al.*,[42] but in the case of linear molecules with more than three atoms, more than one pair of degenerate modes contributes to out-of-plane vibration. In general, one of the vibrational degrees of freedom may be treated as a rotation, but factoring out this degree of freedom rotates the angular coordinate of each degenerate vibration. We will discuss this problem in detail in Sec. II D, and consequences for the full-dimensional Franck-Condon propensities will be discussed in Paper II[72] of this series. Weber and Hohlneicher[47] have calculated multi-dimensional Franck-Condon factors for the acetylene $\tilde{A}$—$\tilde{X}$ transition, but their calculation constrains the molecule to planarity, so they have not considered a number of the symmetry properties and propensity rules that we investigate here in our full-dimensional treatment. They have also rotated the linear molecule to the CC-axis of the trans-bent configurations, so their calculation is inconsistent with Watson's treatment of axis-switching effects.[46,48] To our knowledge, the work presented here is the first publication of a full-dimensional Franck-Condon calculation for a tetra-atomic molecule undergoing a linear-to-bent geometry change.

II. METHODOLOGY FOR THE CALCULATIONS

A. Vibrational intensity factors: Dependence of the electronic transition dipole moment on nuclear coordinates

In the Born-Oppenheimer approximation, the intensity factor S_{ev} accompanying a dipole-allowed vibronic transition is proportional to

$$S_{ev} \propto \sum_{\alpha=a,b,c} |\langle \Psi'_{vib}|\langle \Psi'_{el}|\mu_\alpha|\Psi''_{el}\rangle|\Psi''_{vib}\rangle|^2. \quad (1)$$

In Eq. (1), the rotational and spin contributions to the dipole transition moment are assumed to be separable and have been factored out of the integral. Ψ_{vib} and Ψ_{el} are the vibrational and electronic parts of wavefunction, and single and double primes are used to denote the upper and lower electronic states, respectively. The summation is over the a, b, and c molecular frame axis components of the dipole moment, $\boldsymbol{\mu}$. If we treat the electronic wavefunctions in the adiabatic Born-Oppenheimer basis, then the components of the integral over the electronic degrees of freedom may be written as

$$\langle \Psi'_{el}|\mu_\alpha|\Psi''_{el}\rangle = \int d\mathbf{r}_{el}\ \Psi'_{el}(\mathbf{r}_{el}, \mathbf{q})\mu_\alpha \Psi''_{el}(\mathbf{r}_{el}, \mathbf{q}), \quad (2)$$

where $\mathbf{r}_{el}$ represents the coordinates of the electrons and $\mathbf{q}$ represents the nuclear coordinates. It is important to note that the Born-Oppenheimer electronic wavefunctions $\Psi_{el}(\mathbf{r}_{el}, \mathbf{q})$ are functions of *both* the electronic *and* nuclear coordinates, because they are defined parametrically as functions of nuclear coordinates. Since the integral in (2) is performed only over the electronic degrees of freedom, but the integrand depends on both the electronic and nuclear degrees of freedom, the resulting electronic transition moment is a function of $\mathbf{q}$, and we may say that (2) is a "partial" integral rather than a complete overlap integral over all degrees of freedom. The electronic transition moment may be expanded in terms of the normal mode coordinates of one of the electronic states,

$$\langle \Psi'_{el}|\mu_\alpha|\Psi''_{el}\rangle = \mu_\alpha^{(0)}(el', el'') + \sum_k \mu_\alpha^{(k)}(el', el'')q_k + \frac{1}{2}\sum_{k,k'} \mu_\alpha^{(k,k')}(el', el'')q_k q_{k'} + \ldots, \quad (3)$$

where the subscript k labels the normal modes. In many cases, the integral in Eq. (1) accumulates over a limited range of nuclear geometries over which $\langle \Psi'_{el}|\mu_\alpha|\Psi''_{el}\rangle$ is approximately constant. In such a case, the contributions from higher-order terms in Eq. (3) are small compared to the contribution from $\mu_\alpha^{(0)}(el', el'')$ and may be ignored. The electronic transition dipole moment may then be separated from the vibrational part of the overlap integral in Eq. (1), and the intensity is proportional to the square of the familiar Franck-Condon overlap integral, multiplied by a constant electronic factor,

$$S_{ev} \propto \sum_\alpha \left|\mu_\alpha^{(0)}(el', el'')\right|^2 |\langle \Psi'_{vib}|\Psi''_{vib}\rangle|^2. \quad (4)$$

Familiar symmetry arguments show that the integral in Eq. (2) has a non-zero leading term (i.e., the transition is "electronically allowed") if we set $\mathbf{q}$ to zero and see that $\Gamma(\Psi'_{el}) \otimes \Gamma(\Psi''_{el}) \supset \Gamma(\mu_\alpha)$.

In the case of acetylene, the $\tilde{A}$—$\tilde{X}$ transition is electronically allowed in the lower symmetry point group C_{2h} common to both states, because $\Gamma(\Psi_{\tilde{A}}) \otimes \Gamma(\Psi_{\tilde{X}}) = A_u \otimes A_g$, which contains $\Gamma(\mu_c) = A_u$. However, the transition is electronically forbidden in the higher symmetry point group $D_{\infty h}$ of the ground electronic state, because the $\tilde{A}\ ^1A_u$ state correlates with $^1\Sigma_u^-$ at the linear configuration and it does not have

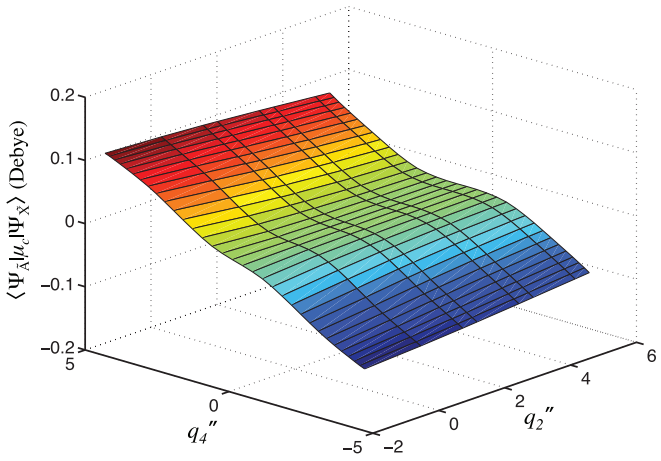

FIG. 1. The value of $\langle\Psi_{\tilde{A}}|\mu_c|\Psi_{\tilde{X}}\rangle$ obtained from the reduced-dimension calculation in Ref. 49 is plotted as a function of q_2'' and q_4''. The normal mode coordinates shown are the dimensionless rectilinear coordinates described in Sec. III. Because the reduced-dimension calculation held the CH bond length fixed to its equilibrium value in the $\tilde{A}$ state, the projection of the data onto the q_2'' coordinate is an approximation that ignores the dependence of q_2'' on the CH bond length.

the correct symmetry to form a totally symmetric product with the $\tilde{X}^1\Sigma_g^+$ state via any of the possible representations of the linear dipole moment operator (Π_u or Σ_u^+). Therefore, $\langle\Psi_{el}'|\boldsymbol{\mu}|\Psi_{el}''\rangle$ approaches zero at the linear configuration and its dependence on nuclear coordinates may *not* be ignored.

We may take the expansion in Eq. (3) about the linear $\tilde{X}$-state equilibrium geometry and employ the $\tilde{X}$-state normal mode coordinates, $\mathbf{q}''$. Since both sides of the equation must have the same symmetry, it is straightforward to determine which terms have the correct symmetry to be non-vanishing. The symmetry of the left-hand side is (from Eq. (2))

$$\begin{aligned}\Gamma(\langle\Psi_{\tilde{A}}|\mu_c|\Psi_{\tilde{X}}''\rangle) &= \Gamma_{el}(\tilde{A})\otimes\Gamma(\mu_c)\otimes\Gamma_{el}(\tilde{X})\\ &= \Sigma_u^-\otimes\Pi_u\otimes\Sigma_g^+\\ &= \Pi_g. \end{aligned}\tag{5}$$

Since the trans-bending mode, ν_4'', is the only normal mode with π_g symmetry, $\mu_c^{(4'')}(\text{el}', \text{el}'')q_4''$ is the only first-order term in the expansion of the electric transition dipole moment about the linear geometry.

Higher-order terms in Eq. (3) with π_g symmetry may also contribute to the integral in Eq. (1), but *ab initio* calculations[49,50] have shown that over the range of geometries relevant to the $\tilde{A}$—$\tilde{X}$ transition, the electronic transition dipole moment is approximately linear in q_4'' and independent of displacement in other modes. The authors of Ref. 49 kindly shared the raw data from their reduced-dimension calculation, performed at the EOM-CCSD level of theory. The dependence of the electronic transition dipole moment on q_2'' and q_4'' obtained from the calculation is shown in Figure 1. From the reduced-dimension data, it was possible to estimate the dependence of $\langle\Psi_{\tilde{A}}|\mu_c|\Psi_{\tilde{X}}\rangle$ on the lowest-order terms in q_2'' and q_4'' (Table I).

In the current work, we ignore higher-order vibrational corrections to the electronic transition dipole moment, and we assume that the vibrational intensity factors are

TABLE I. Lowest-order contributions of q_2'' and q_4'' to the polynomial expansion of $\langle\Psi_{\tilde{A}}|\mu_c|\Psi_{\tilde{X}}\rangle = \sum_{n,m} c_{nm}(q_2'')^n(q_4'')^m$, obtained from a fit to the reduced-dimension calculation from Ref. 49, plotted in Figure 1. Second-order terms in q_2'' were omitted because their contribution was negligible. Values in parentheses represent 2 standard deviations in the uncertainty of the last digit of the fit parameter. The RMS error of the fit to the 256 grid points shown in Figure 1 was 0.0025 D.

n	m	c_{nm} (Debye)
0	1	0.0138(7)
1	1	−0.0026(2)
0	3	0.00109(7)
1	3	$8.3(6)\times10^{-5}$

proportional to

$$S_{ev} \propto |\langle\Psi_{vib}'|q_4''|\Psi_{vib}''\rangle|^2.\tag{6}$$

Watson has shown that including a factor of q_4'' in intensity calculations produces better agreement with experimental absorption data for the $\tilde{A}(v_3') \leftarrow \tilde{X}(0_0)$ progression (see Table 1 of Ref. 46).

B. Nuclear-coordinate dependence of the electronic transition dipole moment in the diabatic picture

It was pointed out to the author by Dr. Josh Baraban that there is an alternative way to describe the dependence of the electronic transition dipole moment on nuclear coordinates using electronic wavefunctions in the diabatic basis. Because the diabatic formulation provides additional insight into the origins of the transition strength, it is presented here briefly. Let Φ_{el} represent a diabatic electronic wavefunction with $D_{\infty h}$ symmetry. Φ_{el} has no explicit dependence on nuclear coordinates, but there may be vibronic interactions that couple electronic states of different symmetry. The $\tilde{X}$ (Σ_g^+) state may have electronically allowed dipole transitions to states of Σ_u^+ or Π_u symmetry. There are no vibrational modes with the correct symmetry to allow a first-order vibronic interaction between the $\tilde{A}$ (Σ_u^-) state and higher-lying Σ_u^+ states, but interactions between the $\tilde{A}$ state and higher-lying Π_u states (such as the $\tilde{C}$ state) may be vibronically mediated by the q_4'' (π_g) vibration. If we assume such an interaction takes place via a matrix element, $H_{12} \propto q_4'' + \ldots$, (the ellipsis indicates higher-order vibrational terms with π_g symmetry that we will ignore), then we may write

$$|\Psi_{\tilde{A}}\rangle = a|\Phi(\Sigma_u^-)\rangle + bq_4''|\Phi(\Pi_u)\rangle,\tag{7}$$

where the a and b mixing coefficients are obtained from diagonalization of the vibronic interaction matrix, and the b coefficient also contains the proportionality of H_{12} to q_4''. The integral in Eq. (1) may then be written as

$$\begin{aligned}S_{ev} &= |\langle\Psi_{vib}'|(a^*\langle\Phi(\Sigma_u^-)| + b^*q_4''\langle\Phi(\Pi_u)|)\mu_c|\Phi_{\tilde{X}}\rangle|\Psi_{vib}''\rangle|^2\\ &= b^2|\langle\Phi(\Pi_u)|\mu_c|\Phi_{\tilde{X}}\rangle|^2|\langle\Psi_{vib}'|q_4''|\Psi_{vib}''\rangle|^2.\end{aligned}\tag{8}$$

Because the diabatic wavefunctions do not depend explicitly on nuclear coordinates, the electronic and vibrational parts of the integral are separable and the first term in the electronic integral vanishes by symmetry. The vibrational q_4'' term that

mediates the vibronic transition is treated in the vibrational integral and we obtain the same result as in Eq. (6).

When viewed in the diabatic picture, it becomes clear that the vibronic mechanism by which the Ã—X̃ becomes electronically allowed is the *same* mechanism that causes the vibronic distortion of the Ã-state equilibrium along the π_g trans-bend coordinate. The dependence of $\langle\Psi_{\tilde{A}}|\mu_c|\Psi_{\tilde{X}}\rangle$ on nuclear coordinates can be directly related to the vibronic distortion of the Ã-state equilibrium because both effects arise from the same matrix element, H_{12}. In the literature, dependence of electronic transition strength on nuclear coordinates (Herzberg-Teller coupling) is often attributed to two seemingly different phenomena: (1) **q**-dependence of the electronic transition dipole moment between the upper and lower electronic states, or (2) intensity borrowing from vibronic interactions. As illustrated by the above example, these two explanations are in fact equivalent descriptions of the same phenomenon, viewed in the basis of (1) adiabatic electronic wavefunctions, or (2) diabatic electronic wavefunctions.

C. Coordinate transformation

Because the normal mode coordinates in the ground and excited states ($\mathbf{q}''$ and $\mathbf{q}'$) are defined differently, $\Psi''_{\rm vib}(\mathbf{q}'')$ and $\Psi'_{\rm vib}(\mathbf{q}')$ are usually given as functions of different sets of variables. In order to evaluate (6) as an overlap integral, a coordinate transformation must be performed to convert the excited-state normal coordinates $\mathbf{q}'$ into ground state coordinates $\mathbf{q}''$. Because the Ã—X̃ transition in acetylene involves a large change in equilibrium geometry between the two electronic states, there are nonlinear contributions to the coordinate transformation. We will consider two different types of corrections. First, we will examine the effects of axis switching between the Cartesian molecular frames of the two states. Next, we examine effects that arise from the curvilinear nature of the normal modes. Either of these corrections might be expected to become important at large displacement along bending coordinates.

1. Axis-switching effects

In the case of acetylene, axis-switching effects[48] accompany the Ã—X̃ transition because the trans↔linear geometry change rotates the orientation of the principal axes about the *c*-axis, and rotation about the *c*-axis is totally symmetric in the C_{2h} point group. Axis-switching effects are most familiar in cases where they give intensity to nominally forbidden rovibronic transitions. For example, axis switching in the Ã—X̃ transition of acetylene gives rise to nominally forbidden *a*-type transitions.[51] However, because axis switching enters into the coordinate transformation, it also plays a role in vibrational intensity factors and its effects should be considered.[52]

In deriving the coordinate transformation appropriate to the acetylene Ã—X̃ transition, Watson includes the effects of axis switching through linear terms in $\mathbf{q}''$.[46] However, Watson's discussion is terse. Therefore, we include some detail about the effects of axis switching on the transformation. In general, the molecular coordinates obeying one set of Eckart conditions may be written in terms of another according to

$$\begin{aligned}\mathbf{r}'_{\mathbf{e}} + \boldsymbol{\rho}' &= \boldsymbol{\Lambda}(\mathbf{r}''_{\mathbf{e}} + \boldsymbol{\rho}'')\\ \boldsymbol{\rho}' &= \boldsymbol{\Lambda}\mathbf{r}''_{\mathbf{e}} - \mathbf{r}'_{\mathbf{e}} + \boldsymbol{\Lambda}\boldsymbol{\rho}'',\end{aligned} \tag{9}$$

where $\mathbf{r}_{\mathbf{e}}$ and $\boldsymbol{\rho}$ are length $3N$ vectors that give the equilibrium position of each nucleus and the displacement of each nucleus from equilibrium, respectively, expressed in the Cartesian principal axis system that satisfies the Eckart conditions for each respective electronic state. Single- and double-primes are used to label the upper and lower electronic states, respectively. The Eckart rotation matrix or "axis-switching" matrix $\boldsymbol{\Lambda}$ in Eq. (9) rotates the principal axis system that obeys the lower state Eckart conditions onto the axis system that obeys the upper state Eckart conditions. The Eckart conditions are satisfied by

$$\mathbf{Q}_{\mathbf{T}} \equiv \tilde{\mathbf{l}}_{\mathbf{T}}\mathbf{m}^{1/2}\boldsymbol{\rho} = M^{-1/2}\sum_i m_i\boldsymbol{\rho}_i = \mathbf{0}, \tag{10}$$

$$\mathbf{Q}_{\mathbf{R}} \equiv \tilde{\mathbf{l}}_{\mathbf{R}}\mathbf{m}^{1/2}\boldsymbol{\rho} = \mathbf{I}^{-1/2}\sum_i m_i(\mathbf{r}_{\mathbf{e},i}\times\boldsymbol{\rho}_i) = \mathbf{0}, \tag{11}$$

where the subscript i labels the nuclei, $M = \sum_i m_i$ is the total mass, and $\mathbf{I}$ is the diagonal moment of inertia tensor for the principal axes. The $3N \times 3N$ diagonal matrix $\mathbf{m}$ weights the Cartesian coordinates by the nuclear masses, and $\tilde{\mathbf{l}}_{\mathbf{R}}$ and $\tilde{\mathbf{l}}_{\mathbf{T}}$ represent the linearized transformations from mass-weighted Cartesian displacements to rotational and translational coordinates, respectively. Throughout this paper, we will use the tilde to denote matrix transposition. The translation of the center of mass may be rigorously separated from other degrees of freedom by condition (10), but the separation of rotational and vibrational coordinates provided by condition (11) is only approximate. Furthermore, because the Eckart conditions (10) and (11) that determine the principal axes are a function of the instantaneous geometry, $\boldsymbol{\Lambda}$ depends on $\mathbf{q}''$ and Eq. (9) is—in general—a nonlinear transformation.

We may write the transformation (9) in terms of vibrational normal mode coordinates using the standard coordinate transformations defined in Ref. 53,

$$\mathbf{Q} = \mathbf{L}_0^{-1}\mathbf{B}_{\mathbf{e}}\boldsymbol{\rho}. \tag{12}$$

Here, $\mathbf{B}_{\mathbf{e}} = (\partial\mathbf{S}/\partial\boldsymbol{\rho})|_{\boldsymbol{\rho}=\mathbf{0}}$ transforms Cartesian displacements to "linearized" internal coordinates, $\mathbf{S}$, and $\mathbf{L}_0^{-1}$ transforms the $\mathbf{S}$ coordinates to normal mode coordinates of dimension $\sqrt{\text{mass}}\cdot\text{distance}$. Because the $\mathbf{B}_{\mathbf{e}}$ matrix is defined in terms of infinitesimal curvilinear displacements from a reference equilibrium geometry, $\mathbf{Q}$ is a linear combination of Cartesian displacements for each nucleus. In this paper, we use scaled dimensionless normal mode vibrational coordinates $\mathbf{q}$ defined according to

$$\mathbf{q} = \boldsymbol{\gamma}^{1/2}\mathbf{Q}, \tag{13}$$

where $\boldsymbol{\gamma}$ is a diagonal scaling matrix with elements $\gamma_k = hc\omega_k/\hbar^2$. ($\omega_k$ is the harmonic frequency of the kth normal mode.) We insert (12) to obtain

$$\begin{aligned}\mathbf{q} &= \boldsymbol{\gamma}^{1/2}\mathbf{L}_0^{-1}\mathbf{B}_{\mathbf{e}}\boldsymbol{\rho}\\ &= \boldsymbol{\gamma}^{1/2}\tilde{\mathbf{l}}\mathbf{m}^{1/2}\boldsymbol{\rho}.\end{aligned} \tag{14}$$

We have introduced the substitution $\mathbf{l} = \mathbf{m}^{-1/2}\tilde{\mathbf{B}}_\mathbf{e}\tilde{\mathbf{L}}_\mathbf{0}^{-1}$. $\tilde{\mathbf{l}}$ is the $3N \times n_{\text{vib}}$ matrix that transforms mass-weighted Cartesian coordinates to normal mode vibrational coordinates, and n_{vib} is the number of vibrational degrees of freedom being considered.

The $3N \times 3N$ matrix that transforms Cartesian coordinates to the $3N$-dimensional vector of normal vibrational, rotational, and translational coordinates according to

$$\begin{bmatrix} \mathbf{Q} \\ \mathbf{Q_R} \\ \mathbf{Q_T} \end{bmatrix} = \begin{bmatrix} \tilde{\mathbf{l}} \\ \tilde{\mathbf{l}}_\mathbf{R} \\ \tilde{\mathbf{l}}_\mathbf{T} \end{bmatrix} \mathbf{m}^{1/2}\boldsymbol{\rho} \tag{15}$$

is a unitary transformation,[53] so

$$\begin{bmatrix} \mathbf{l}\ \mathbf{l}_\mathbf{R}\ \mathbf{l}_\mathbf{T} \end{bmatrix} \begin{bmatrix} \mathbf{Q} \\ \mathbf{Q_R} \\ \mathbf{Q_T} \end{bmatrix} = \mathbf{m}^{1/2}\boldsymbol{\rho}. \tag{16}$$

We may now write the coordinate transformation (9) in terms of normal coordinates by substituting (15) and (16) for $\boldsymbol{\rho}'$ and $\boldsymbol{\rho}''$ to obtain

$$\begin{bmatrix} \mathbf{Q}' \\ \mathbf{Q}'_\mathbf{R} \\ \mathbf{Q}'_\mathbf{T} \end{bmatrix} = \begin{bmatrix} \tilde{\mathbf{l}}' \\ \tilde{\mathbf{l}}'_\mathbf{R} \\ \tilde{\mathbf{l}}'_\mathbf{T} \end{bmatrix} \mathbf{m}^{1/2}(\boldsymbol{\Lambda}\mathbf{r}''_\mathbf{e} - \mathbf{r}'_\mathbf{e}) + \begin{bmatrix} \tilde{\mathbf{l}}'\boldsymbol{\Lambda}\mathbf{l}'' & \tilde{\mathbf{l}}'\boldsymbol{\Lambda}\mathbf{l}''_\mathbf{R} & \tilde{\mathbf{l}}'\boldsymbol{\Lambda}\mathbf{l}''_\mathbf{T} \\ \tilde{\mathbf{l}}'_\mathbf{R}\boldsymbol{\Lambda}\mathbf{l}'' & \tilde{\mathbf{l}}'_\mathbf{R}\boldsymbol{\Lambda}\mathbf{l}''_\mathbf{R} & \tilde{\mathbf{l}}'_\mathbf{R}\boldsymbol{\Lambda}\mathbf{l}''_\mathbf{T} \\ \tilde{\mathbf{l}}'_\mathbf{T}\boldsymbol{\Lambda}\mathbf{l}'' & \tilde{\mathbf{l}}'_\mathbf{T}\boldsymbol{\Lambda}\mathbf{l}''_\mathbf{R} & \tilde{\mathbf{l}}'_\mathbf{T}\boldsymbol{\Lambda}\mathbf{l}''_\mathbf{T} \end{bmatrix} \begin{bmatrix} \mathbf{Q}'' \\ \mathbf{Q}''_\mathbf{R} \\ \mathbf{Q}''_\mathbf{T} \end{bmatrix}. \tag{17}$$

We enforce the Eckart conditions by setting $\mathbf{Q_R} = \mathbf{Q_T} = \mathbf{0}$ for both states to obtain the set of equations

$$\mathbf{q}' = (\boldsymbol{\gamma}')^{1/2}\,\tilde{\mathbf{l}}'[\boldsymbol{\Lambda}\mathbf{m}^{1/2}\mathbf{r}''_\mathbf{e} - \mathbf{m}^{1/2}\mathbf{r}'_\mathbf{e}] + (\boldsymbol{\gamma}')^{1/2}\,\tilde{\mathbf{l}}'\boldsymbol{\Lambda}\mathbf{l}''(\boldsymbol{\gamma}'')^{-1/2}\mathbf{q}'', \tag{18}$$

$$\tilde{\mathbf{l}}'_\mathbf{R}\boldsymbol{\Lambda}\left[\mathbf{m}^{1/2}\mathbf{r}''_\mathbf{e} + \mathbf{l}''(\boldsymbol{\gamma}'')^{1/2}\mathbf{q}''\right] = \mathbf{0}. \tag{19}$$

We have used the fact that $\tilde{\mathbf{l}}'_\mathbf{R}\mathbf{m}^{1/2}\mathbf{r}'_\mathbf{e} = \mathbf{0}$ because the equilibrium geometry satisfies the Eckart condition (11). Equation (18) is the desired (nonlinear) coordinate transformation. The first term in Eq. (18) accounts for the difference in equilibrium geometry of the upper and lower states and the second term accounts for displacement of molecular geometry away from the lower state equilibrium. Equation (19) enforces the rotational Eckart condition (11) for each state. Equation (19) may be used to define $\boldsymbol{\Lambda}$ as a function of $\mathbf{q}''$. We have omitted the equation for the translational Eckart condition, obtained from the third row of Eq. (17). It is trivially zero since condition (10) ensures that the origin of the principal axis system for each state is at the center of mass.

In order to expand the transformation (18) to first-order in $\mathbf{q}''$, we define

$$\boldsymbol{\Lambda} = \boldsymbol{\Lambda}_\mathbf{e}(\mathbf{E} + \boldsymbol{\Lambda}_\mathbf{1}(\mathbf{q}'')), \tag{20}$$

where $\mathbf{E}$ is the unit matrix. $\boldsymbol{\Lambda}_\mathbf{e}$ is the axis-switching matrix that satisfies Eq. (19) at the lower state equilibrium and the dependence of the axis rotation on $\mathbf{q}''$ is contained in $\boldsymbol{\Lambda}_\mathbf{1}$. For small displacements, we may use the infinitesimal rotation matrix,

$$\boldsymbol{\Lambda}_\mathbf{1} \approx \begin{bmatrix} 0 & \mathrm{d}\Omega_c & -\mathrm{d}\Omega_b \\ -\mathrm{d}\Omega_c & 0 & \mathrm{d}\Omega_a \\ \mathrm{d}\Omega_b & -\mathrm{d}\Omega_a & 0 \end{bmatrix}. \tag{21}$$

Note that the effect of $\boldsymbol{\Lambda}_\mathbf{1}$ operating on a vector $\mathbf{r}$ may be written as a cross product

$$\boldsymbol{\Lambda}_\mathbf{1}\mathbf{r} = \mathbf{r} \times \mathbf{d}\vec{\boldsymbol{\Omega}}, \tag{22}$$

where $\mathbf{d}\vec{\boldsymbol{\Omega}}$ is the vector $\langle \mathrm{d}\Omega_a\ \mathrm{d}\Omega_b\ \mathrm{d}\Omega_c \rangle$. Thus by the definition in (11), the rotation of the equilibrium Cartesian coordinates $\boldsymbol{\Lambda}_\mathbf{1}\mathbf{m}^{1/2}\mathbf{r}_\mathbf{e}$ is related to the rotation matrix $\tilde{\mathbf{l}}_\mathbf{R}$ by

$$\begin{aligned} \boldsymbol{\Lambda}_\mathbf{1}\mathbf{m}^{1/2}\mathbf{r}_\mathbf{e} &= \mathbf{m}^{1/2}\mathbf{r}_\mathbf{e} \times \mathbf{d}\vec{\boldsymbol{\Omega}} \\ &= \mathbf{I}_\mathbf{e}{}^{1/2}\mathbf{l}_\mathbf{R}\mathbf{d}\vec{\boldsymbol{\Omega}}, \end{aligned} \tag{23}$$

where $\mathbf{I}_\mathbf{e}$ denotes the moment of inertia tensor at the equilibrium configuration. We now substitute Eqs. (20), (22), and (23) into the Eckart condition (19) for the transformation and solve for $\mathbf{d}\vec{\boldsymbol{\Omega}}$, noting that $\tilde{\mathbf{l}}'_\mathbf{R}\boldsymbol{\Lambda}_\mathbf{e}\mathbf{m}^{1/2}\mathbf{r}''_\mathbf{e} = \mathbf{0}$, because the $\boldsymbol{\Lambda}_\mathbf{e}$ rotation satisfies the upper state Eckart conditions for $\mathbf{q}'' = \mathbf{0}$:

$$\begin{aligned} \mathbf{d}\vec{\boldsymbol{\Omega}} = -\left[\tilde{\mathbf{l}}'_\mathbf{R}\boldsymbol{\Lambda}_\mathbf{e}(\mathbf{I}_\mathbf{e}'')^{1/2}\mathbf{l}_\mathbf{R}{}''\right]^{-1}\left[\tilde{\mathbf{l}}'_\mathbf{R}\boldsymbol{\Lambda}_\mathbf{e}\mathbf{l}''(\boldsymbol{\gamma}'')^{1/2}\mathbf{q}'' \right. \\ \left. + \tilde{\mathbf{l}}'_\mathbf{R}\boldsymbol{\Lambda}_\mathbf{e}\boldsymbol{\Lambda}_\mathbf{1}\mathbf{l}''(\boldsymbol{\gamma}'')^{1/2}\mathbf{q}''\right]. \end{aligned} \tag{24}$$

The second term in (24) is $O[(\mathbf{q}'')^2]$ and may be ignored in the first-order expansion.

We now substitute (20) and (24) into the coordinate transformation (18), and use the relation (23) to obtain (noting that the factors of $(\mathbf{I}''_\mathbf{e})^{1/2}$ cancel)

$$\mathbf{q}' = \boldsymbol{\delta}^{(\text{a-s})} + \mathbf{D}^{(\text{a-s})}\mathbf{q}'' + O[(\mathbf{q}'')^2], \tag{25}$$

$$\boldsymbol{\delta}^{(\text{a-s})} = (\boldsymbol{\gamma}')^{1/2}\left[\tilde{\mathbf{l}}'\boldsymbol{\Lambda}_\mathbf{e}\mathbf{m}^{1/2}\mathbf{r}''_\mathbf{e} - \tilde{\mathbf{l}}'\mathbf{m}^{1/2}\mathbf{r}'_\mathbf{e}\right], \tag{26}$$

$$\mathbf{D}^{(\text{a-s})} = (\boldsymbol{\gamma}')^{1/2}\left[\tilde{\mathbf{l}}'\boldsymbol{\Lambda}_\mathbf{e}\mathbf{l}'' - \tilde{\mathbf{l}}'\boldsymbol{\Lambda}_\mathbf{e}\mathbf{l}''_\mathbf{R}(\tilde{\mathbf{l}}'_R\boldsymbol{\Lambda}_\mathbf{e}\mathbf{l}''_\mathbf{R})^{-1}\tilde{\mathbf{l}}'_R\boldsymbol{\Lambda}_\mathbf{e}\mathbf{l}''\right](\boldsymbol{\gamma}'')^{-1/2}, \tag{27}$$

$$O[(\mathbf{q}'')^2] \approx (\boldsymbol{\gamma}')^{1/2}\tilde{\mathbf{l}}'\boldsymbol{\Lambda}_\mathbf{e}[\mathbf{E} + \mathbf{l}''_\mathbf{R}(\tilde{\mathbf{l}}'_R\boldsymbol{\Lambda}_\mathbf{e}\mathbf{l}''_\mathbf{R})^{-1}\tilde{\mathbf{l}}'_\mathbf{R}\boldsymbol{\Lambda}_\mathbf{e}]\boldsymbol{\Lambda}_\mathbf{1}\mathbf{l}''(\boldsymbol{\gamma}'')^{-1/2}\mathbf{q}''. \tag{28}$$

The $\boldsymbol{\delta}^{(\text{a-s})}$ vector gives the upper state normal mode coordinates at the equilibrium geometry of the lower state (the shift of origin), and may have nonzero elements for totally symmetric normal modes in the point group common to both states. The $\mathbf{D}^{(\text{a-s})}$ matrix describes (to first order) the transformation of lower state normal mode coordinates to upper state normal mode coordinates. It is block-diagonal with respect to the symmetries of the normal modes. Off-diagonal elements allow "Duschinski rotation" between normal modes of the same symmetry.[38] The "(a-s)" superscript denotes that the transformation takes into account first-order corrections for axis-switching. The first term in (27) gives the zero-order projection of the ground-state normal modes onto the basis of the excited-state normal modes after rotating the equilibrium ground-state principal axes into the excited-state Eckart frame. The second term is a first-order correction term for the

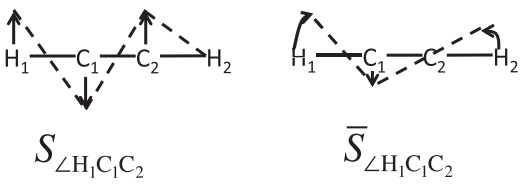

FIG. 2. The rectilinear internal coordinate $S_{\angle H_1C_1C_2}$ stretches the bond lengths in acetylene, while the curvilinear internal coordinate $\bar{S}_{\angle H_1C_1C_2}$ changes only the HCC bond angle while other bond angles and lengths remain constant.

dependence of the Eckart conditions on the instantaneous geometry. Equations (25)–(27) are equivalent to Eqs. (8)–(10) of Ref. 46. Higher order corrections to the transformation arising from the terms in (28) are considered by Özkan,[52] but will be ignored in the present work.

2. Curvilinear effects

The normal mode coordinates $\mathbf{Q}$, defined by Eq. (12), are rectilinear in the sense that displacement along any given mode (all other normal mode displacements held constant), results in straight-line motion of each nucleus in the molecular coordinate frame. This is because each normal mode is defined as a linear combination of "linearized" internal coordinates, $\mathbf{S}$. A classic paper by Hoy, Mills, and Strey[54] describes the transformation to the true curvilinear internal coordinates (which we will denote $\bar{\mathbf{S}}$), defined in terms of the bond lengths and angles. As shown in Figure 2, the rectilinear bending coordinate $S_{\angle H_1C_1C_2}$ stretches the C—H bond at large displacements from the linear equilibrium.

In many cases, it is useful to work with rectilinear normal coordinates because they provide a convenient simplification of the kinetic energy operator,

$$T_{\text{kin}} = \frac{1}{2}\frac{\mathrm{d}\tilde{\mathbf{S}}}{\mathrm{d}t}\left(\tilde{\mathbf{B}}_{\mathbf{e}}^{-1}\mathbf{m}\mathbf{B}_{\mathbf{e}}^{-1}\right)\frac{\mathrm{d}\mathbf{S}}{\mathrm{d}t} = \frac{1}{2}\frac{\mathrm{d}\tilde{\mathbf{Q}}}{\mathrm{d}t}\frac{\mathrm{d}\mathbf{Q}}{\mathrm{d}t}.$$

As we will see below, curvilinear coordinates *do not* afford the same simplification and their use comes at the price of higher-order terms in the kinetic energy operator. Nevertheless, for problems involving large amplitude bending motion, it is sometimes simpler to work in the basis of curvilinear normal modes. For example, Borrelli and Peluso[55,56] have shown that the use of curvilinear coordinates has a profound simplifying effect on the coordinate transformation for the $V \leftarrow N$ transition in ethylene, which involves a 90° twist along the torsional coordinate. The reason for this simplification is that curvilinear coordinates reduce cross-anharmonicities introduced between stretching and bending coordinates, as illustrated in Figure 2.

The potential energy may be expanded in either coordinate system,

$$V = \frac{1}{2}\sum_{ij} f^{ij}S_iS_j + \frac{1}{6}\sum_{ijk} f^{ijk}S_iS_jS_k + \frac{1}{24}\sum_{ijkl} f^{ijkl}S_iS_jS_kS_l\ldots \tag{29}$$

$$= \frac{1}{2}\sum_{ij} \phi^{ij}\bar{S}_i\bar{S}_j + \frac{1}{6}\sum_{ijk} \phi^{ijk}\bar{S}_i\bar{S}_j\bar{S}_k + \frac{1}{24}\sum_{ijkl} \phi^{ijkl}\bar{S}_i\bar{S}_j\bar{S}_k\bar{S}_l\ldots. \tag{30}$$

In general, the coefficients in the two expansions are different. However, because the leading quadratic terms that determine the harmonic force field depend only on infinitesimal displacements, for which $\mathbf{S}$ and $\bar{\mathbf{S}}$ are identical, $\phi^{ij} = f^{ij}$, and we see that in the harmonic limit the coordinate systems are interchangeable and the distinction is moot. However, at large displacements from equilibrium, curvilinear coordinates often provide a simpler description of the potential energy because the potential energy surface of most molecules tends to be steepest along directions that stretch or contract the bond lengths. As a result the force field naturally tends to send nuclei along curved bending trajectories, and the curvilinear cross-anharmonicities $\phi^{ijk\cdots}$ may be much smaller in magnitude than $f^{ijk\cdots}$.

Several authors have discussed approximate methods for using curvilinear coordinates in the Franck-Condon coordinate transformation.[57–59] The transformation from curvilinear $\bar{\mathbf{S}}$ to rectilinear $\mathbf{Q}$ is nonlinear.

$$\bar{S}_i = L_i^r Q_r + \frac{1}{2}L_i^{rs}Q_rQ_s + \frac{1}{6}L_i^{rst}Q_rQ_sQ_t + \ldots, \tag{31}$$

where $L_i^r = (\partial\bar{S}_i/\partial Q_r)|_{\bar{S}=0}$ are elements of the $\mathbf{L_0}$ matrix defined in Sec. II C 1, and higher-order components of the $\mathbf{L}$ tensor define the nonlinear transformation. We may define curvilinear normal coordinates, $\bar{\mathbf{Q}}$, by truncating the expansion in (31),

$$\bar{S}_i = L_i^r\bar{Q}_r, \quad \text{or} \quad \bar{\mathbf{Q}} \equiv \mathbf{L}_0^{-1}\bar{\mathbf{S}}. \tag{32}$$

As shown by Capobianco and co-workers,[58] the quantum vibrational Hamiltonian may then be written as

$$\hat{H} = \hat{H}_0^{(\text{c-l})} + \Delta T_{\text{kin}} + V_{\text{kin}}(\bar{\mathbf{Q}}) + \Delta V(\bar{\mathbf{Q}}), \tag{33}$$

where $\hat{H}_0^{(\text{c-l})}$ is the harmonic Hamiltonian written in curvilinear normal coordinates,

$$\hat{H}_0^{(\text{c-l})} = -\frac{\hbar^2}{2}\sum_r \frac{\partial^2}{\partial\bar{Q}_r^2} + \frac{1}{2}\sum_r \omega_r^2\bar{Q}_r^2, \tag{34}$$

and the remaining terms are

$$\Delta T_{\text{kin}} = \frac{\hbar}{2}\sum_{jk}\frac{\partial^2}{\partial\bar{Q}_j\partial\bar{Q}_k} - \frac{\hbar^2}{2}\sum_{jk}\frac{\partial}{\partial\bar{Q}_j}g_{jk}(\bar{\mathbf{Q}})\frac{\partial}{\partial\bar{Q}_k}, \tag{35}$$

$$V_{\rm kin}(\bar{\mathbf{Q}}) = \frac{5\hbar}{32g^2}\sum_{jk} g_{jk}\frac{\partial g}{\partial \bar{Q}_j}\frac{\partial g}{\partial \bar{Q}_k} - \frac{\hbar^2}{8g}\sum_{jk}\frac{\partial g_{jk}}{\partial \bar{Q}_j}\frac{\partial g}{\partial \bar{Q}_k} - \frac{\hbar^2}{8g}\sum_{jk} g_{jk}\frac{\partial^2 g}{\partial \bar{Q}_j \partial \bar{Q}_k}, \quad (36)$$

and $\Delta V(\bar{\mathbf{Q}})$ collects the anharmonic potential energy terms. $g_{jk}(\bar{\mathbf{Q}})$ and g are the matrix elements and the determinant, respectively, of

$$\mathbf{g} = \mathbf{L}_0^{-1}\mathbf{B}(\bar{\mathbf{Q}})\mathbf{m}^{-1}\tilde{\mathbf{B}}(\bar{\mathbf{Q}})\tilde{\mathbf{l}}_0^{-1}. \quad (37)$$

In (37), $\mathbf{B}(\bar{\mathbf{Q}})$ is the transformation $\mathbf{B}(\bar{\mathbf{Q}}) = (\partial\bar{\mathbf{S}}/\partial\boldsymbol{\rho})$, which depends on the instantaneous vibrational coordinates. The zero order expansion of $g_{jk}(\bar{\mathbf{Q}})$ in the second term of (35) is unity and cancels the first term, so that the leading term of $\Delta T_{\rm kin}$ is third-order in the position and momentum operators.

In the basis set of the eigenfunctions of $\hat{H}_0^{\rm (c\text{-}l)}$, the coordinate transformation between $\bar{\mathbf{q}}'' = (\boldsymbol{\gamma}'')^{1/2}\bar{\mathbf{Q}}''$ and $\bar{\mathbf{q}}' = (\boldsymbol{\gamma}')^{1/2}\bar{\mathbf{Q}}'$ is given by

$$\bar{\mathbf{q}}' = \mathbf{D}^{\rm (c\text{-}l)}\bar{\mathbf{q}}'' + \boldsymbol{\delta}^{\rm (c\text{-}l)}, \quad (38)$$

$$\mathbf{D}^{\rm (c\text{-}l)} = (\boldsymbol{\gamma}')^{1/2}(\mathbf{L}_0')^{-1}(\mathbf{L}_0'')(\boldsymbol{\gamma}'')^{-1/2}, \quad (39)$$

$$\boldsymbol{\delta}^{\rm (c\text{-}l)} = (\boldsymbol{\gamma}')^{1/2}(\mathbf{L}_0')^{-1}(\boldsymbol{\zeta}_e{}'' - \boldsymbol{\zeta}_e{}'), \quad (40)$$

where $\boldsymbol{\zeta}_e{}'$ and $\boldsymbol{\zeta}_e{}''$ are the equilibrium values of the internal coordinates in the upper and lower state, respectively, about which the displacements $\bar{\mathbf{S}} = \boldsymbol{\zeta} - \boldsymbol{\zeta}_e$ are defined, and the superscript (c-l) indicates that the transformation is performed in the basis of curvilinear harmonic oscillators. A transformation is given conveniently in terms of the Cartesian $\mathbf{l}$ matrices by Reimers,[57]

$$\boldsymbol{\delta}^{\rm (c\text{-}l)} = (\boldsymbol{\gamma}')^{1/2}\tilde{\mathbf{l}}'\mathbf{m}^{-1/2}\tilde{\mathbf{B}}_0'(\mathbf{B}_0'\mathbf{m}^{-1}\tilde{\mathbf{B}}_0')^{-1}, \quad (41)$$

$$\mathbf{D}^{\rm (c\text{-}l)} = (\boldsymbol{\gamma}')^{1/2}\tilde{\mathbf{l}}'\mathbf{m}^{-1/2}\tilde{\mathbf{B}}_0'(\mathbf{B}_0'\mathbf{m}^{-1}\tilde{\mathbf{B}}_0')^{-1/2} \times (\mathbf{B}_0''\mathbf{m}^{-1}\tilde{\mathbf{B}}_0'')^{-1/2}\tilde{\mathbf{B}}_0''\mathbf{m}^{-1/2}\mathbf{l}''(\boldsymbol{\gamma}'')^{-1/2}. \quad (42)$$

Both of the transformations that we have presented—(25)–(28) and (38)–(42)—are analogous to Eq. (10) of Sharp and Rosenstock,[40] in the limit of small displacements. If the displacement in equilibrium geometry between the two electronic states is small then $\boldsymbol{\Lambda} \approx \mathbf{E}$, and axis switching effects do not enter into the coordinate transformation. Similarly, if only small displacements along the normal mode coordinates are considered, then the curvilinear $\bar{\mathbf{q}}$ are equivalent to the rectilinear $\mathbf{q}$ and $\tilde{\mathbf{l}}'\mathbf{l}'' \approx (\mathbf{L}_0')^{-1}(\mathbf{L}_0'')$. The reader should be cautioned that the paper by Sharp and Rosenstock contains typographical errors.[40] Care must be taken to correct the errors when applying equations from that paper. Some of the errata have been published in Ref. 60. Corrected versions of key equations from Ref. 40 are also printed in Ref. 47.

D. Coordinate transformation for bent—linear transitions

Some additional complications are presented by the $\tilde{\rm A}$—$\tilde{\rm X}$ transition in acetylene because the ground state has a linear equilibrium geometry while the electronically-excited $\tilde{\rm A}$-state is trans-bent. In the most familiar formulation of the rovibrational Hamiltonian, states with nonlinear equilibrium geometry are treated with 3 rotational degrees of freedom and $3N-6$ vibrational degrees of freedom, while states with linear equilibrium geometry are treated with 2 rotational degrees of freedom and $3N-5$ vibrational degrees of freedom. In this formulation for linear molecules, the 3-dimensional moment of inertia tensor is singular and all angular momentum about the a-inertial axis arises from vibration.

For the current problem of full-dimensional Franck–Condon factors in the acetylene $\tilde{\rm A}$—$\tilde{\rm X}$ system, it is more convenient to formulate the $\tilde{\rm X}$-state Hamiltonian in terms of 3 rotational degrees of freedom and $3N-6$ vibrational degrees of freedom. Watson has discussed in detail the formulation of the rovibrational kinetic energy operator for this case, and the reader is referred to Ref. 61.

The (x, y) sub-block of $\mathbf{I}$ is trivially diagonal in the linear configuration. Therefore, in the conventional treatment involving only two rotations, the χ Euler angle is not defined. Rotation of the molecular orientation around the z-axis is instead achieved by a rotation of the polar coordinates of each of the degenerate bending modes, q_t, which are defined relative to the x and y axes by

$$q_{tx}^u = \rho_t \cos\phi_t^u, \quad (43)$$

$$q_{ty}^u = \rho_t \sin\phi_t^u, \quad (44)$$

where t is an index that labels the bending vibrational modes, and the u superscript signifies that the polar coordinates are unconstrained. To add a third rotational degree of freedom (restoring χ), a constraint must be placed on the vibrational coordinates so that the total number of degrees of freedom remains constant. In general, the constraint may be accomplished by choosing a nonlinear reference configuration, $\mathbf{q}_{\rm ref}$, and then restricting the polar coordinates ϕ_t of the degenerate bending modes to locate the x and y axes such that the (x, y) block of the moment of inertia tensor is diagonal. This allows reintroduction of the χ Euler angle to give constrained polar angles ϕ_t according to

$$\phi_t = \phi_t^u - \chi. \quad (45)$$

In the case of a linear–nonlinear transition, the natural choice of reference configuration is the equilibrium geometry of the nonlinear state, so for the current problem, we choose as the reference configuration the trans-bent $\tilde{\rm A}$-state equilibrium geometry. The off-diagonal element of the (x, y) block of $\mathbf{I}$ is

$$I_{xy} = -\sum_i m_i r_{ix} r_{iy}, \quad (46)$$

where (r_{ix}, r_{iy}) is the (x, y) position of the ith nucleus in the trans-bent reference configuration (and the orientation of the x and y axes are to be defined by the constraint). Only the trans- and cis-bending modes (ν_4'' and ν_5'', respectively) have amplitude in the (x, y) plane, and furthermore, the displacement along the *ungerade* cis bend, q_5'', is zero at the centrosymmetric $\tilde{\rm A}$-state equilibrium. Therefore, q_4'' will be the only contribution to r_{ix} and r_{iy}. Since the requirement $I_{xy} = 0$ satisfies the Eckart conditions, we have from Eq. (16)

$m_i^{1/2} r_{ix} = l''_{ix,4}(\gamma''_4)^{-1/2} q''_{4x}$ and $m_i^{1/2} r_{iy} = l''_{iy,4}(\gamma''_4)^{-1/2} q''_{4y}$, so

$$I_{xy} = -q''_{4x} q''_{4y} \sum_i \left(\frac{l''_{ix,4} l''_{iy,4}}{\gamma''_4} \right) = 0, \tag{47}$$

or, from Eqs. (43) and (44)

$$-\frac{1}{2}\rho''_4 \sin 2\phi_4 = 0. \tag{48}$$

Equation (48) has more than one solution, but it is conventional to choose y to correspond with the out-of-plane c-axis in the trans C_{2h} configuration, so we choose the solution $\phi_4 = 0$, (or $q''_{4y} = 0$), which gives

$$\chi = \phi_4^u, \tag{49}$$

$$\phi_5 = \phi_5^u - \chi. \tag{50}$$

The resulting constraint ensures that displacement along q''_4 must lie in the plane of the equilibrium geometry of the trans-bent $\tilde{A}$ state. Note that constraining ϕ_4 to zero and restoring the χ Euler angle is equivalent to removing the $\exp(il_4\phi_4)$ factor from the two-dimensional harmonic oscillator wavefunction and including it instead in the rotational integral. Hence, the $(v - l)/2$ radial nodes of the two-dimensional harmonic oscillator wavefunction for mode ν''_4 are included in the vibrational FC factor, but the angular factor is not. On the other hand, ϕ_5 is *not* constrained to zero, so it will contribute both a radial and angular factor to the vibrational integral. This leads to important propensity rules and symmetry considerations for the vibrational overlap integrals, which will be discussed in Paper II[72] of this series. Some of these considerations have been neglected by other authors because they have not considered the problem of linear-to-bent transitions in full dimension.

The rotational integral may be evaluated from the μ_c matrix elements. Formulas for rotational strength factors for linear to bent transitions are given in Ref. 62. In the current work, we ignore rovibrational interactions and we are primarily interested with the vibrational intensity factors rather than the distribution of that intensity between the rotational states within each vibrational band, so we have ignored the rotational integral.

E. Method of generating functions

1. General case for nonlinear molecules

The method of generating functions used by Sharp and Rosenstock for calculating Franck-Condon overlap integrals makes use of the exponential generating function for Hermite polynomials (denoted $H_v(q)$)

$$\exp(2sq - s^2) = \sum_v \frac{H_v(q) s^v}{v!}. \tag{51}$$

To generate properly normalized wavefunctions $\langle q|v\rangle$ of the dimensionless variable $q = (hc\omega/\hbar^2)^{1/2} Q$, we use

$$\sum_v \frac{\langle q|v\rangle s^v}{\sqrt{v!}} = \pi^{-\frac{1}{4}} \exp\left(-\frac{1}{2}q^2 + \sqrt{2}sq - \frac{1}{2}s^2 \right), \tag{52}$$

$$\langle q|v\rangle = \pi^{-\frac{1}{4}} \left(\frac{1}{2^v v!} \right)^{\frac{1}{2}} \exp\left(\frac{-q^2}{2} \right) H_v(q). \tag{53}$$

Equation (52) states that if we take the exponential function on the right-hand side and expand it as a polynomial of the dummy variable s, then we obtain the Harmonic oscillator wavefunctions as coefficients. Any desired Harmonic oscillator wavefunction, $\langle q|v\rangle$, may be obtained by collecting the coefficient of s to the desired power. The factor of $\sqrt{v!}$ in the denominator is required in order to achieve the properly normalized wavefunction given in Eq. (53). Note that in Eq. (52), s has been scaled by a factor of $2^{-1/2}$ to achieve the factor of $2^{(-v/2)}$ in the normalization constant of Eq. (53).

To generate an n_{vib}-dimensional harmonic oscillator wavefunction in the product basis, $\langle \mathbf{q}|\mathbf{v}\rangle = \prod_k \langle q_k|v_k\rangle$, we may write Eq. (52) in terms of the vector $\mathbf{q}$ and use a dummy vector $\mathbf{s}$ of length n_{vib},

$$\sum_{\mathbf{v}} \frac{\langle \mathbf{q}|\mathbf{v}\rangle \prod_k s_k^{v_k}}{\prod_k (v_k!)^{1/2}} = \pi^{-n_{vib}/4} \exp\left(-\frac{1}{2}\tilde{\mathbf{q}}\mathbf{q} + \sqrt{2}\tilde{\mathbf{s}}\mathbf{q} - \frac{1}{2}\tilde{\mathbf{s}}\mathbf{s} \right), \tag{54}$$

where k is an index that labels each mode and the summation over $\mathbf{v}$ on the left-hand side denotes summation over each v_k.

To obtain the overlap integral in Eq. (4), we wish to calculate

$$\langle \Psi'_{vib}|\Psi''_{vib}\rangle = \int \left| \frac{\partial \mathbf{q}'}{\partial \mathbf{q}''} \right|^{\frac{1}{2}} d\mathbf{q}'' \ \langle \mathbf{v}'|\mathbf{q}'\rangle \langle \mathbf{q}''|\mathbf{v}''\rangle, \tag{55}$$

where $\int d\mathbf{q}''$ is shorthand for $\int_{-\infty}^{\infty} \dots \int_{-\infty}^{\infty} \prod_k dq''_k$. The $|\partial \mathbf{q}'/\partial \mathbf{q}''|$ represents the determinant of the matrix of partial derivatives with components $D_{ij} = \partial q'_i/\partial q''_j$. It is included because the transformation $\mathbf{q}' = \mathbf{D}\mathbf{q}'' + \boldsymbol{\delta}$ need not be unitary, and the wavefunction $\Psi'_{vib}(\mathbf{q}')$ must therefore be renormalized by the Jacobian determinant for integration with respect to $\mathbf{q}''$:

$$\int d\mathbf{q}' |\Psi'_{vib}(\mathbf{q}')|^2 = 1 \tag{56}$$

$$\int \left| \frac{\partial \mathbf{q}'}{\partial \mathbf{q}''} \right| d\mathbf{q}'' |\Psi'_{vib}(\mathbf{q}'')|^2 = 1 \tag{57}$$

$$\det(\mathbf{D}) \int d\mathbf{q}'' |\Psi'_{vib}(\mathbf{q}'')|^2 = 1. \tag{58}$$

We define renormalized excited-state wavefunctions $\Psi''^{(rn)}_{vib}(\mathbf{q}'') = \sqrt{\det(\mathbf{D})}\, \Psi'_{vib}(\mathbf{q}'')$, so that

$$\int d\mathbf{q}'' \left| \Psi''^{(rn)}_{vib}(\mathbf{q}'') \right|^2 = 1. \tag{59}$$

We obtain a generating function G for Eq. (55) by taking the product of Eq. (54) for the ground and excited states and

performing the integral with respect to $d\mathbf{q}''$:

$$G = \sum_{\mathbf{v}',\mathbf{v}''} \frac{\langle \mathbf{v}'|\mathbf{v}''\rangle \prod_{k',k''} (s_{k'})^{v'_{k'}} (t_{k''})^{v''_{k''}}}{\prod_{k',k''} [(v'_{k'}!)(v''_{k''}!)]^{1/2}}$$
$$= \left(\frac{\det \mathbf{D}}{\pi^{n_{\text{vib}}}}\right)^{\frac{1}{2}} \int d\mathbf{q}'' \exp\left(-\frac{1}{2}\tilde{\mathbf{q}}'\mathbf{q}' + \sqrt{2}\,\tilde{\mathbf{s}}\mathbf{q}' - \frac{1}{2}\tilde{\mathbf{s}}\mathbf{s}\right)$$
$$\times \exp\left(-\frac{1}{2}\tilde{\mathbf{q}}''\mathbf{q}'' + \sqrt{2}\,\tilde{\mathbf{t}}\mathbf{q}'' - \frac{1}{2}\tilde{\mathbf{t}}\mathbf{t}\right). \quad (60)$$

We have used $s_{k'}$ as the dummy variable for the excited state modes and $t_{k''}$ as the dummy variable for the ground state modes. We substitute $\mathbf{q}' = \mathbf{D}\mathbf{q}'' + \boldsymbol{\delta}$ to obtain

$$G = \left(\frac{\det \mathbf{D}}{\pi^{n_{\text{vib}}}}\right)^{\frac{1}{2}} \exp\left(-\frac{1}{2}\tilde{\boldsymbol{\delta}}\boldsymbol{\delta} + \sqrt{2}\tilde{\mathbf{s}}\boldsymbol{\delta} - \frac{1}{2}\tilde{\mathbf{s}}\mathbf{s} - \frac{1}{2}\tilde{\mathbf{t}}\mathbf{t}\right)$$
$$\times \int d\mathbf{q}'' \exp\left[-\tilde{\mathbf{q}}''\mathbf{A}\mathbf{q}'' + (\sqrt{2}\tilde{\mathbf{s}}\mathbf{D} + \sqrt{2}\tilde{\mathbf{t}} - \tilde{\boldsymbol{\delta}}\mathbf{D})\mathbf{q}''\right]. \quad (61)$$

We have made the substitution $\mathbf{A} = \frac{1}{2}(\mathbf{E} + \tilde{\mathbf{D}}\mathbf{D})$, where $\mathbf{E}$ is the $n_{\text{vib}} \times n_{\text{vib}}$ identity matrix. The integral in Eq. (61) can be solved by changing coordinates to the basis that diagonalizes $\mathbf{A}$ and evaluating the resulting one-dimensional Gaussian integrals. Note that $\mathbf{A}$ is a symmetric matrix and therefore guaranteed to be diagonalizable by an orthogonal matrix. Let $\mathbf{V}$ be the orthogonal matrix that diagonalizes $\mathbf{A}$ such that $\tilde{\mathbf{V}}\mathbf{A}\mathbf{V} = \boldsymbol{\Theta}$, ($\boldsymbol{\Theta}$ is diagonal), and let $\mathbf{y}$ be the transformation of $\mathbf{q}''$ under $\mathbf{V}$ so that $\tilde{\mathbf{V}}\mathbf{q}'' = \mathbf{y}$. Since $\mathbf{V}$ is orthogonal (and unitary), the Jacobian determinant of the transformation is unity and $d\mathbf{q}'' = d\mathbf{y}$.

Substituting $\mathbf{q}'' = \mathbf{V}\mathbf{y}$, we obtain

$$G = \left(\frac{\det \mathbf{D}}{\pi^{n_{\text{vib}}}}\right)^{\frac{1}{2}} \exp\left(-\frac{1}{2}\tilde{\boldsymbol{\delta}}\boldsymbol{\delta} + \sqrt{2}\tilde{\mathbf{s}}\boldsymbol{\delta} - \frac{1}{2}\tilde{\mathbf{s}}\mathbf{s} - \frac{1}{2}\tilde{\mathbf{t}}\mathbf{t}\right)$$
$$\times \int d\mathbf{y} \exp\left(-\tilde{\mathbf{y}}\boldsymbol{\Theta}\mathbf{y} + \tilde{\mathbf{w}}\mathbf{y}\right), \quad (62)$$

where we have substituted $\tilde{\mathbf{w}} = (\sqrt{2}\tilde{\mathbf{s}}\mathbf{D} + \sqrt{2}\tilde{\mathbf{t}} - \tilde{\boldsymbol{\delta}}\mathbf{D})\mathbf{V}$. Since $\boldsymbol{\Theta}$ is diagonal, the integral in (62) may be evaluated as a product of one-dimensional Gaussian integrals:

$$G = \left(\frac{\det \mathbf{D}}{\pi^{n_{\text{vib}}}}\right)^{\frac{1}{2}} \exp\left(-\frac{1}{2}\tilde{\boldsymbol{\delta}}\boldsymbol{\delta} + \sqrt{2}\tilde{\mathbf{s}}\boldsymbol{\delta} - \frac{1}{2}\tilde{\mathbf{s}}\mathbf{s} - \frac{1}{2}\tilde{\mathbf{t}}\mathbf{t}\right)$$
$$\times \prod_i^{n_{\text{vib}}} \int dy_i \exp\left(-\Theta_{ii} y_i^2 + w_i y_i\right)$$
$$= \left(\frac{\det \mathbf{D}}{\pi^{n_{\text{vib}}}}\right)^{\frac{1}{2}} \exp\left(-\frac{1}{2}\tilde{\boldsymbol{\delta}}\boldsymbol{\delta} + \sqrt{2}\tilde{\mathbf{s}}\boldsymbol{\delta} - \frac{1}{2}\tilde{\mathbf{s}}\mathbf{s} - \frac{1}{2}\tilde{\mathbf{t}}\mathbf{t}\right)$$
$$\times \prod_i^{n_{\text{vib}}} \sqrt{\frac{\pi}{\Theta_{ii}}} \exp\left(\frac{w_i^2}{4\Theta_{ii}}\right)$$
$$= \left(\frac{\det \mathbf{D}}{\det \boldsymbol{\Theta}}\right)^{\frac{1}{2}} \exp\left(-\frac{1}{2}\tilde{\boldsymbol{\delta}}\boldsymbol{\delta} + \sqrt{2}\tilde{\mathbf{s}}\boldsymbol{\delta} - \frac{1}{2}\tilde{\mathbf{s}}\mathbf{s} - \frac{1}{2}\tilde{\mathbf{t}}\mathbf{t}\right)$$
$$\times \exp\left(\frac{1}{4}\tilde{\mathbf{w}}\Theta^{-1}\mathbf{w}\right).$$

After some algebra, we find

$$\frac{1}{4}\tilde{\mathbf{w}}\boldsymbol{\Theta}^{-1}\mathbf{w} = \frac{1}{4}(\sqrt{2}\tilde{\mathbf{s}} - \tilde{\boldsymbol{\delta}})(2\mathbf{E} - \mathbf{B}^{-1})(\sqrt{2}\mathbf{s} - \boldsymbol{\delta})$$
$$+ \frac{1}{\sqrt{2}}(\sqrt{2}\tilde{\mathbf{s}} - \tilde{\boldsymbol{\delta}})\mathbf{X}^{-1}\mathbf{t} + \frac{1}{2}\tilde{\mathbf{t}}\mathbf{A}^{-1}\mathbf{t}, \quad (63)$$

where we have made the substitutions

$$\mathbf{B} = \frac{1}{2}(\mathbf{E} + \mathbf{D}\tilde{\mathbf{D}}) = \mathbf{D}\mathbf{A}\mathbf{D}^{-1} = (2\mathbf{E} - \mathbf{D}\mathbf{A}^{-1}\tilde{\mathbf{D}})^{-1}, \quad (64)$$

$$\mathbf{X} = \frac{1}{2}(\tilde{\mathbf{D}} + \mathbf{D}^{-1}) = \mathbf{A}\mathbf{D}^{-1} = \mathbf{D}^{-1}\mathbf{B}, \quad (65)$$

and where $\mathbf{E}$ represents the $n_{\text{vib}} \times n_{\text{vib}}$ identity matrix. We also note that $\det \boldsymbol{\Theta} = \det \mathbf{A}$ because the determinant is invariant under a unitary transformation. The final expression for G is

$$G = \sum_{\mathbf{v}',\mathbf{v}''} \frac{\langle \mathbf{v}'|\mathbf{v}''\rangle \prod_{k',k''} (s_{k'})^{v'_{k'}} (t_{k''})^{v''_{k''}}}{\prod_{k',k''} [(v'_{k'}!)(v''_{k''}!)]^{1/2}}$$
$$= \left(\frac{1}{\det \mathbf{X}}\right)^{\frac{1}{2}} \exp\left(-\frac{1}{4}\tilde{\boldsymbol{\delta}}\mathbf{B}^{-1}\boldsymbol{\delta}\right)$$
$$\times \exp\left[\frac{1}{2}\tilde{\mathbf{s}}(\mathbf{E} - \mathbf{B}^{-1})\mathbf{s} - \frac{1}{2}\tilde{\mathbf{t}}\left(\mathbf{E} - \mathbf{A}^{-1}\right)\mathbf{t} + \tilde{\mathbf{s}}\mathbf{X}^{-1}\mathbf{t}\right.$$
$$\left. + \frac{1}{\sqrt{2}}\tilde{\mathbf{s}}\mathbf{B}^{-1}\boldsymbol{\delta} - \frac{1}{\sqrt{2}}\tilde{\boldsymbol{\delta}}\mathbf{X}^{-1}\mathbf{t}\right]. \quad (66)$$

This is in agreement with the equation obtained by Watson[46] and the corrected version of the equation obtained by Sharp and Rosenstock.[40,60]

2. Generating function for the full-dimensional acetylene $\tilde{A}$—$\tilde{X}$ system

Watson has derived a generating function for the *gerade* modes of the acetylene $\tilde{A}$—$\tilde{X}$ system.[46] It is our goal here to extend Watson's work to obtain a full-dimensional treatment. Watson treats the doubly degenerate bending mode ν_4'' in the (v, l)-basis and integrates the wavefunction in polar coordinates, ρ_4, ϕ_4. He makes use of the generating function

$$\sqrt{\frac{\rho_t}{\pi}} \exp\left\{-\frac{1}{2}\rho_t + \frac{1}{\sqrt{2}}\rho_t e^{i\phi_t} su + \frac{1}{\sqrt{2}}\rho_t e^{-i\phi_t} su^{-1} - \frac{1}{2}s^2\right\}$$
$$= \sum_{v_t,l_t} \frac{\langle \rho_t\phi_t|v_t l_t\rangle s^{v_t} u^{l_t}}{\left\{2^{v_t}\left[\frac{1}{2}(v_t + l_t)\right]!\left[\frac{1}{2}(v_t - l_t)\right]!\right\}^{1/2}}. \quad (67)$$

In Eq. (67), l_t is a signed quantity ($-v_t \le l_t \le v_t$) so the right-hand side is *not* a polynomial in the dummy variable u. The wavefunctions obtained from this generating function may be written explicitly as

$$\langle \rho_t\phi_t|v_t l_t\rangle = \frac{(-1)^{(3v_t+l_t)/2}}{\sqrt{\pi}} \left(\frac{\left[\frac{1}{2}(v_t - l_t)\right]!}{\left[\frac{1}{2}(v_t + l_t)\right]!}\right)^{1/2}$$
$$\times \rho_t^{(l_t+1/2)} e^{-\rho_t^2/2} L^{l_t}_{\frac{1}{2}(v_t-l_t)}(\rho_t^2) e^{il_t\phi_t}, \quad (68)$$

where $L_n^{\alpha}(x)$ represents the associated Laguerre polynomial. Note that Eq. (68) differs from the form of the wavefunction

given in most textbooks by a factor of $\rho_t^{1/2}$. This factor is included to normalize the wavefunctions with respect to integration over polar coordinates,

$$\int\int \mathrm{d}\rho_t \mathrm{d}\phi_t \langle v_t' l_t' | \rho_t \phi_t \rangle \langle \rho_t \phi_t | v_t l_t \rangle = \delta_{v_t', v_t} \delta_{l_t', l_t}. \tag{69}$$

To obtain a generating function for the Franck-Condon overlap integrals of doubly degenerate bending modes in the linear ground state of acetylene, we may substitute the left-hand side of Eq. (67) for the appropriate normal mode dimensions in the second exponential of Eq. (60). In treating the *gerade* modes, Watson makes use of the Euler angle constraint $\phi_4 = 0$ and makes the substitution $u_4 = \exp(i\psi_4)$, which simplifies the resulting integral. The factor of $\exp(i\phi_4'')$ is treated as part of the rotational wavefunction.

In the full-dimensional treatment of FC factors for the $\tilde{\mathrm{A}}$—$\tilde{\mathrm{X}}$ acetylene transition, however, there are *two* doubly degenerate bending modes that must be treated, ν_4'' and ν_5''. If we were to use a generating function for the ν_5'' wavefunctions of the type presented in Eq. (67), we would have to integrate over ϕ_5 and the exponential term in the integral would no longer be separable into a product of one-dimensional Gaussian integrals. Therefore, in order to simplify the integral in the current work, we choose to represent ν_5'' in the (v_x, v_y) basis and to use generating functions of the type presented in Eq. (52). We leave ν_4'' in the (v, l) basis to take advantage of the simplifications afforded by the Euler angle constraint on ϕ_4. Finally, we include an extra factor of ρ_4'' to capture the linear dependence on ρ_4'' of the transition dipole moment, as in Eq. (6). The resulting generating function is

$$\begin{aligned} G = {} & (\det \mathbf{D})^{1/2} \int \mathbf{dq}'' \pi^{-5/4} \exp\left(-\frac{1}{2}\tilde{\mathcal{Q}}''\mathcal{Q}'' + \sqrt{2}\tilde{\mathcal{T}}\mathcal{Q}'' - \frac{1}{2}\tilde{\mathcal{T}}\mathcal{T}\right) \\ & \times \pi^{-1/2} (\rho_4'')^{3/2} \exp\left(-\frac{1}{2}(\rho_4'')^2 + \frac{2}{\sqrt{2}}\rho_4'' t_4 \cos\psi_4 - \frac{1}{2}t_4^2\right) \\ & \times \pi^{-3/2} \exp\left(-\frac{1}{2}\tilde{\mathbf{q}}'\mathbf{q}' + \sqrt{2}\tilde{\mathbf{s}}\mathbf{q}' - \frac{1}{2}\tilde{\mathbf{s}}\mathbf{s}\right) \\ = {} & \sum_{\mathbf{v}', \mathbf{v}'', l_4''} \frac{\langle \mathbf{v}' | \mathbf{v}'', l_4'' \rangle \prod_{k',k''} s_{k'}^{v_{k'}'} t_{k''}^{v_{k''}''}}{(v_1'! v_2'! v_3'! v_4'! v_5'! v_6'!)^{1/2} (v_1''! v_2''! v_3''! v_{5x}''! v_{5y}''!)^{1/2}} \\ & \times \frac{\cos l_4'' \psi_4}{\left\{2^{v_4''}\left[\frac{1}{2}(v_4'' + l_4'')\right]!\left[\frac{1}{2}(v_4'' - l_4'')\right]!\right\}^{1/2}}, \end{aligned} \tag{70}$$

where

$$\begin{aligned} \mathbf{dq}'' &= \mathrm{d}q_1'' \mathrm{d}q_2'' \mathrm{d}q_3'' \mathrm{d}\rho_4'' \mathrm{d}q_{5x}'' \mathrm{d}q_{5y}'', \\ \tilde{\mathcal{Q}}'' &= (q_1'', q_2'', q_3'', q_{5x}'', q_{5y}''), \\ \tilde{\mathcal{T}} &= (t_1, t_2, t_3, t_{5x}, t_{5y}), \end{aligned}$$

and $\tilde{\mathbf{q}}'$ and $\tilde{\mathbf{s}}'$ are (1×6) row vectors with one element for each excited-state normal mode. The limits of integration with respect to $\mathrm{d}\rho_4''$ are $(0, \infty)$, and all other limits of integration are $(-\infty, \infty)$. After substituting $\mathbf{q}' = \mathbf{D}\mathbf{q}'' + \boldsymbol{\delta}$ into Eq. (70), we obtain

$$\begin{aligned} G = {} & \pi^{-13/4} (\det \mathbf{D})^{1/2} \int \mathbf{dq}'' (\rho_4'')^{3/2} \\ & \times \exp\left[-\tilde{\mathbf{q}}''\mathbf{A}\mathbf{q}'' + (-\tilde{\boldsymbol{\delta}}\mathbf{D} + \sqrt{2}\tilde{\mathbf{s}}\mathbf{D} + \sqrt{2}\tilde{\mathbf{T}})\mathbf{q}'' \right. \\ & \left. - \frac{1}{2}\tilde{\boldsymbol{\delta}}\boldsymbol{\delta} + \sqrt{2}\tilde{\mathbf{s}}\boldsymbol{\delta} - \frac{1}{2}\tilde{\mathbf{s}}\mathbf{s} - \frac{1}{2}\tilde{\mathbf{t}}\mathbf{t}\right], \end{aligned} \tag{71}$$

where

$$\tilde{\mathbf{q}}'' = (q_1'', q_2'', q_3'', \rho_4'', q_{5x}'', q_{5y}''), \tag{72}$$

$$\tilde{\mathbf{t}} = (t_1, t_2, t_3, t_4, t_{5x}, t_{5y}), \tag{73}$$

$$\tilde{\mathbf{T}} = (t_1, t_2, t_3, t_4 \cos\phi_4, t_{5x}, t_{5y}). \tag{74}$$

The integral in Eq. (71) differs from the one in Eq. (60) because it includes a factor of $(\rho_4'')^{3/2}$, and the limits of integration with respect to ρ_4'' are $(0, \infty)$. These considerations make it difficult to perform the change of variables as we did in Sec. II E 1. As mentioned in Sec. II A, the electronic transition dipole moment for the $\tilde{\mathrm{A}}$—$\tilde{\mathrm{X}}$ transition in acetylene vanishes at the linear configuration, so most of the overlap integral accumulates at configurations away from linearity ($\rho_4'' \neq 0$). Following Watson, we can use Laplace's approximation for the integral in Eq. (71), as follows. If $h(\mathbf{x})$ and $g(\mathbf{x})$ are real-valued functions and $g(\mathbf{x})$ has a single absolute maximum at $\mathbf{x_0}$ in the domain of integration, F, $g(\mathbf{x_0}) = \max[g(\mathbf{x})]$, then

$$\begin{aligned} & \int_F \mathbf{dx}\, h(\mathbf{x}) \exp(M g(\mathbf{x})) \\ & \approx \left(\frac{2\pi}{M}\right)^{\frac{n}{2}} \left(\frac{1}{|\det[\mathbf{H}_g(\mathbf{x_0})]|}\right)^{\frac{1}{2}} h(\mathbf{x_0}) \exp(M g(\mathbf{x_0})), \end{aligned} \tag{75}$$

where M is a real number, n is the length of the vector $\mathbf{x}$, and $\mathbf{H}_g(\mathbf{x_0})$ is the Hessian matrix of second derivatives of $g(\mathbf{x})$, evaluated at $\mathbf{x_0}$. Equation (75) is valid in the limit $M \to \infty$ and is an exact solution for the Gaussian case where $h(\mathbf{x})$ is constant, $g(\mathbf{x})$ is quadratic with negative second partial derivatives, and the limits of integration are $(-\infty, \infty)$ for all variables. Laplace's approximation is a good strategy for the integral in Eq. (71) because it would provide the exact solution if it were not for the $(\rho_4'')^{3/2}$ factor and the limits of integration with respect to ρ_4'', so in a sense it is an approximation only for a single coordinate. Furthermore, because the Franck-Condon overlap is expected to accumulate mostly at bending geometries intermediate to the $\tilde{\mathrm{A}}$- and $\tilde{\mathrm{X}}$-state equilibria, we expect this approximation to be valid with respect to the ρ_4'' coordinate.

We apply Eq. (75) to the integral in Eq. (71), letting $h(\mathbf{x}) = (\rho_4'')^{3/2}$, $M = 1$, and $g(\mathbf{x})$ equal the argument of the exponential in Eq. (71). We first find the value of $\mathbf{q}''$ that maximizes g. We note that since $\mathbf{A}$ is a symmetric matrix,

$$\frac{\partial}{\partial \mathbf{q}''} \tilde{\mathbf{q}}''\mathbf{A}\mathbf{q}'' = 2\mathbf{A}\mathbf{q}''. \tag{76}$$

We differentiate the exponential in (71) to obtain

$$\frac{\partial}{\partial \mathbf{q}''}\left[-\tilde{\mathbf{q}}''\mathbf{A}\mathbf{q}'' + (-\tilde{\boldsymbol{\delta}}\mathbf{D} + \sqrt{2}\tilde{\mathbf{s}}D + \sqrt{2}\tilde{\mathbf{T}})\mathbf{q}'' - \frac{1}{2}\tilde{\boldsymbol{\delta}}\boldsymbol{\delta} + \sqrt{2}\tilde{\mathbf{s}}\boldsymbol{\delta} - \frac{1}{2}\tilde{\mathbf{s}}\mathbf{s} - \frac{1}{2}\tilde{\mathbf{t}}\mathbf{t}\right]\Big|_{\mathbf{q}_0''} = 0$$

$$-2\mathbf{A}\mathbf{q}_0'' - \tilde{\mathbf{D}}\boldsymbol{\delta} + \sqrt{2}\tilde{\mathbf{D}}\mathbf{s} + \sqrt{2}\mathbf{T} = 0. \tag{77}$$

Thus,

$$\mathbf{q}_0'' = \frac{1}{2}\mathbf{A}^{-1}(-\tilde{\mathbf{D}}\boldsymbol{\delta} + \sqrt{2}\tilde{\mathbf{D}}\mathbf{s} + \sqrt{2}\mathbf{T}). \tag{78}$$

The value of ρ_4'' at the maximum of the argument of the exponential is the fourth element of the vector equation (78),

$$(\rho_4'')_0 = [\mathbf{q}_0'']_4 = \left[\frac{1}{2}\mathbf{A}^{-1}(-\tilde{\mathbf{D}}\boldsymbol{\delta} + \sqrt{2}\tilde{\mathbf{D}}\mathbf{s} + \sqrt{2}\mathbf{T})\right]_4. \tag{79}$$

We can now substitute Eqs. (78) and Eq. (79) into Eq. (75), noting that $\mathbf{H}_g(\mathbf{q}_0'') = 2\mathbf{A}$. After some algebra, we obtain

$$G = \pi^{-\frac{1}{4}}(\det \mathbf{X})^{-\frac{1}{2}}(\rho_4'')_0^{3/2} \times \exp\left[\frac{1}{2}\tilde{\mathbf{s}}(\mathbf{E} - \mathbf{B}^{-1})\mathbf{s} - \frac{1}{2}\tilde{\mathbf{t}}\mathbf{t} + \frac{1}{2}\tilde{\mathbf{T}}\mathbf{A}^{-1}\mathbf{T} + \tilde{\mathbf{s}}\mathbf{X}^{-1}\mathbf{T} + \frac{\sqrt{2}}{2}\tilde{\mathbf{s}}\mathbf{B}^{-1}\boldsymbol{\delta} - \frac{\sqrt{2}}{2}\tilde{\boldsymbol{\delta}}\mathbf{X}^{-1}\mathbf{T} - \frac{1}{4}\tilde{\boldsymbol{\delta}}\mathbf{B}^{-1}\boldsymbol{\delta}\right]$$

$$= \sum_{\mathbf{v}',\mathbf{v}'',l_4''} \frac{\langle \mathbf{v}'|\mathbf{v}'', l_4''\rangle \prod_{k',k''}(s_{k'})^{v_{k'}'}(t_{k''})^{v_{k''}''}}{(v_1'!v_2'!v_3'!v_4'!v_5'!v_6'!)^{1/2}(v_1''!v_2''!v_3''!v_{5x}''!v_{5y}''!)^{1/2}} \times \frac{\cos l_4''\psi_4}{\left\{2^{v_4''}\left[\frac{1}{2}(v_4'' + l_4'')\right]!\left[\frac{1}{2}(v_4'' - l_4'')\right]!\right\}^{1/2}}. \tag{80}$$

This equation has the same form as that derived by Watson (Eq. (29) of Ref. 46), except for the definitions of **s**, **t**, and **T**. Also, we have not included the factor of $(2 - \delta_{l_4'',0})$, which Watson uses to account for the degeneracy of states with $|l_4''| = \pm l_4''$. In the current work, we are interested applying our Franck-Condon calculation to cases in which states differing only in ± parity may be resolved or in which transitions to only one of the parity components is allowed.

3. Change of basis for ν_5''

The generating function in Eq. (80) calculates overlap integrals for the cis-bending mode ν_5'' in the $|v_{5x}'', v_{5y}''\rangle$ basis, but for most spectroscopic applications, we wish to work in the $|v_5'', l_5''\rangle$ basis. A state in the $|v_5'', l_5''\rangle$ basis may be expressed as a linear combination of states in the $|v_{5x}'', v_{5y}''\rangle$ basis with $v_{5x}'' + v_{5y}'' = v_5''$,

$$|\{\boldsymbol{\alpha}''\}, v_5'', l_5''\rangle = \sum_{i=0}^{v_5''} c_i |\{\boldsymbol{\alpha}''\}, v_{5x}'' = v_5 - i, v_{5y}'' = i\rangle, \tag{81}$$

where $\{\boldsymbol{\alpha}''\}$ represents a given set of values for all other quantum numbers of the state. Therefore, the Franck-Condon overlap integral in the $|v_5'', l_5''\rangle$ basis may be expressed as a linear combination of Franck-Condon overlap integrals in the $|v_{5x}'', v_{5y}''\rangle$ basis with the same coefficients:

$$\langle \mathbf{v}'|\{\boldsymbol{\alpha}''\}, v_5'', l_5''\rangle = \sum_{i=0}^{v_5''} c_i \langle \mathbf{v}'|\{\boldsymbol{\alpha}''\}, v_{5x}'' = v_5'' - i, v_{5y}'' = i\rangle. \tag{82}$$

The coefficients c_i may be obtained by applying 2-dimensional harmonic oscillator raising and lowering operators found in many quantum mechanics textbooks, such as Ref. 63. Briefly, the coefficients may be obtained by expanding the operator equation

$$|v, l\rangle = \frac{1}{\sqrt{[(v+l)/2]![(v-l)/2]!}}\left(\hat{a}_x^\dagger + i\hat{a}_y^\dagger\right)^{(v+l)/2} \times \left(\hat{a}_x^\dagger - i\hat{a}_y^\dagger\right)^{(v-l)/2}|0, 0\rangle, \tag{83}$$

and evaluating terms on the right-hand side according to

$$\left(\hat{a}_x^\dagger\right)^{n_x}\left(\hat{a}_y^\dagger\right)^{n_y}|0, 0\rangle = \sqrt{n_x!n_y!}\,|n_x, n_y\rangle. \tag{84}$$

TABLE II. Normal mode labels for $\tilde{X}$-state acetylene. The harmonic vibrational frequencies (taken from Ref. 26) were determined from experiment after deperturbing the anharmonic resonances.

Mode	Description	Symmetry	ω/cm^{-1}
ν_1''	Symmetric stretch	σ_g^+	3397.12
ν_2''	CC stretch	σ_g^+	1981.80
ν_3''	Antisymmetric stretch	σ_u^+	3316.86
ν_4''	Trans bend	π_g	608.73
ν_5''	Cis bend	π_u	729.08

III. CALCULATION OF COORDINATE TRANSFORMATION PARAMETERS FOR THE $\tilde{A}$—$\tilde{X}$ SYSTEM OF ACETYLENE

The normal mode frequencies and symmetries of the $\tilde{X}$ and $\tilde{A}$ states are summarized in Tables II and III. Parameters for the $\tilde{X}$-state equilibrium geometry and harmonic force field used in the evaluation of the coordinate transformation were taken from Halonen *et al.* ("Model II" of the paper).[65] In order to reproduce the results of Watson, we first used the $\tilde{A}$-state geometry and harmonic force field from Tobiason *et al.*[66] Using these force fields, we obtained elements for the *gerade* block of $\mathbf{D}^{(a\text{-}s)}$ and $\boldsymbol{\delta}^{(a\text{-}s)}$ that agree with those obtained by Watson to within a phase factor of ±1.[46] The phase factor

TABLE III. Normal mode labels for $\tilde{A}$-state acetylene. The harmonic vibrational frequencies (taken from Ref. 64) were determined from experiment after deperturbing the anharmonic resonances.

Mode	Description	Symmetry	ω/cm^{-1}
ν_1'	Symmetric stretch	a_g	3052.1
ν_2'	CC stretch	a_g	1420.9
ν_3'	Trans bend	a_g	1098.0
ν_4'	Torsion	a_u	787.7
ν_5'	Antisymmetric stretch	b_u	3032.4
ν_6'	Cis bend	b_u	801.6

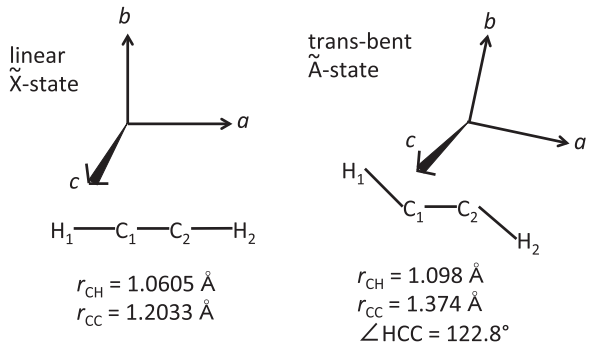

FIG. 3. The labeling of the acetylene nuclei and the orientation of the principal inertial axis system used in the construction of **l** matrices. The *c*-axis points out of the page towards the viewer. The equilibrium geometries used in the calculation are also shown.

of ±1 reflects the fact that Watson uses a different phase convention for the columns of the **l** matrices. The choice of phase convention will not affect the magnitude of individual Franck-Condon factors between harmonic oscillator basis states, but may affect the relative signs of the overlap integrals. Therefore, if we wish to be able to calculate interference effects arising from admixture of harmonic oscillator basis states involved in the initial and final states of a given transition, we must ensure that the phase convention used to define the normal modes given by the columns of the **l** matrix is consistent with the phases used to determine the signs of the matrix elements between the basis states. In the current work, we have chosen the columns of $\mathbf{l}''$ to be consistent with the parameters of the X̃-state effective Hamiltonian reported by Herman and co-workers[21,23] and expanded by Jacobson and co-workers.[24,28,67] The columns of $\mathbf{l}'$ are chosen to have positive overlap with the corresponding columns of $\mathbf{l}''$. We have chosen $\mathbf{l}''_{\mathbf{R}}$ and $\mathbf{l}'_{\mathbf{R}}$ so that positive displacement corresponds to right-handed rotation around the axes as defined in Figure 3.

Recent spectral analysis published since the Tobiason *et al.* force field[66] has uncovered new parameters relevant to the force field of the Ã-state of acetylene. Most notably, the fundamental frequencies ν'_1 of $^{12}C_2H_2$ (Ref. 34) and ν'_2 and ν'_3 of $^{13}C_2H_2$ (Ref. 64) have been found and a complete set of $^{12}C_2H_2$ x_{ij} cross anharmonicities has now been determined.[30,34–36,68–70] Jiang *et al.* have recently reported an updated force field for the Ã-state that takes the large amount of new data into account.[64] We have used the updated force field from "Fit Method I" in Ref. 64 (Column 1 of Table 6 in the reference) in our determination of the coordinate transformations reported below.

The **l** matrices (Tables IV and V) were obtained by diagonalizing the **FG** matrix as described by Wilson, Decius and Cross,[53] and the $\mathbf{l}_{\mathbf{R}}$ matrices are calculated from

$$(\mathbf{l}_{\mathbf{R}})_{i\alpha,\beta} = \sum_{\gamma\delta} e_{\alpha\gamma\delta} m_i^{1/2} (\mathbf{r}_{\mathbf{e}})_{i\delta} (\mathbf{I}_{\mathbf{e}}^{-1/2})_{\gamma\beta}, \tag{85}$$

where the *i* subscript refers to the *i*th nucleus, Greek letter subscripts refer to Cartesian directions, $e_{\alpha\gamma\delta}$ is the antisymmetric unit tensor, and $\mathbf{I}_{\mathbf{e}}$ is the moment of inertia tensor evaluated at the equilibrium geometry. The equilibrium Eckart rotation matrix is then obtained by solving Eq. (19) at the equilibrium X̃-state geometry ($\mathbf{q}'' = \mathbf{0}$). That is,

$$\tilde{\mathbf{l}}'_{\mathbf{R}} \boldsymbol{\Lambda}_{\mathbf{e}} \mathbf{m}^{1/2} \mathbf{r}''_{\mathbf{e}} = \mathbf{0}. \tag{86}$$

In order to illustrate the effects of axis-switching and curvilinear modes on the coordinate transformation, we first report the zeroth-order transformation (Table VI), obtained from

$$\boldsymbol{\delta}^{(0)} = (\boldsymbol{\gamma}')^{1/2} \left[\tilde{\mathbf{l}}' \mathbf{m}^{1/2} \mathbf{r}''_{\mathbf{e}} - \tilde{\mathbf{l}}' \mathbf{m}^{1/2} \mathbf{r}'_{\mathbf{e}} \right], \tag{87}$$

$$\mathbf{D}^{(0)} = (\boldsymbol{\gamma}')^{1/2} \tilde{\mathbf{l}}' \mathbf{l}'' (\boldsymbol{\gamma}'')^{-1/2}. \tag{88}$$

Next, we report corrections to the zeroth-order transformation. The coordinate transformation with first-order correction for axis-switching effects is calculated from Eqs. (26) and (27), and the parameters are tabulated in Table VII. The geometry change results in an equilibrium Eckart rotation of

TABLE IV. Elements of the $\mathbf{l}''$ and $\mathbf{l}''_{\mathbf{R}}$ matrices for the X̃ state of acetylene evaluated using the force field of Ref. 65.

	$\mathbf{l}''$						$\mathbf{l}''_{\mathbf{R}}$		
	q''_1	q''_2	q''_{4b}	q''_3	q''_{5b}	q''_{5c}	R''_a (q''_{4c})	R''_b	R''_c
a_{H_1}	−0.6420	−0.2964	0	−0.6791	0	0	0	0	0
b_{H_1}	0	0	0.5520	0	0.6792	0	0	0	−0.4419
c_{H_1}	0	0	0	0	0	0.6792	0.5520	0.4419	0
a_{C_1}	0.2964	−0.6420	0	0.1968	0	0	0	0	0
b_{C_1}	0	0	−0.4419	0	−0.1968	0	0	0	−0.5520
c_{C_1}	0	0	0	0	0	−0.1968	−0.4419	0.5520	0
a_{C_2}	−0.2964	0.6420	0	0.1968	0	0	0	0	0
b_{C_2}	0	0	0.4419	0	−0.1968	0	0	0	0.5520
c_{C_2}	0	0	0	0	0	−0.1968	0.4419	−0.5520	0
a_{H_2}	0.6420	0.2964	0	−0.6792	0	0	0	0	0
b_{H_2}	0	0	−0.5520	0	0.6792	0	0	0	0.4419
c_{H_2}	0	0	0	0	0	0.6792	−0.5520	−0.4419	0

TABLE V. Elements of the $\mathbf{l}'$ and $\mathbf{l}'_{\mathbf{R}}$ matrices for the $\tilde{A}$ state of acetylene evaluated using the force field of Jiang *et al.*[64]

	$\mathbf{l}'$						$\mathbf{l}'_{\mathbf{R}}$		
	q'_1	q'_2	q'_3	q'_5	q'_6	q'_4	R'_a	R'_b	R'_c
a_{H_1}	−0.4757	−0.1970	0.4539	−0.4804	0.4812	0	0	0	−0.1695
b_{H_1}	0.4811	0.0150	0.3787	0.4801	0.4804	0	0	0	−0.3535
c_{H_1}	0	0	0	0	0	0.6792	0.6036	0.3683	0
a_{C_1}	0.1630	−0.6750	−0.0836	0.1392	−0.1391	0	0	0	0.1035
b_{C_1}	−0.1251	−0.0720	−0.3789	−0.1391	−0.1392	0	0	0	−0.5792
c_{C_1}	0	0	0	0	0	−0.1968	−0.3683	0.6036	0
a_{C_2}	−0.1629	0.6751	0.0836	0.1392	−0.1391	0	0	0	−0.1034
b_{C_2}	0.1252	0.0721	0.3789	−0.1391	−0.1392	0	0	0	0.5793
c_{C_2}	0	0	0	0	0	−0.1968	0.3683	−0.6036	0
a_{H_2}	0.4758	0.1971	−0.4539	−0.4804	0.4812	0	0	0	0.1696
b_{H_2}	−0.4810	−0.0150	−0.3787	0.4801	0.4793	0	0	0	0.3535
c_{H_2}	0	0	0	0	0	0.6792	−0.6036	−0.3683	0

−2.143° about the *c*-axis. The coordinate transformation in the basis of curvilinear normal mode coordinates is calculated from Eqs. (41) and (42), and the parameters are tabulated in Table VIII.

Inspection of the parameters tabulated in Tables VI–VIII reveals the relative magnitudes of the corrections to the zeroth-order coordinate transformation. Axis-switching has a relatively strong effect (∼10%) on the shift of origin for ν'_1, and a weaker effect on the Duschinsky rotation of in-plane vibrational modes. The first order correction term (the second term in Eq. (27)) only affects the Duschinsky rotation in the totally symmetric a_g block of **D**, because rotation about the *c*-axis has the same symmetry as a_g vibration, which leads to a first-order interaction between axis switching and a_g vibration. The first order correction decreases the Duschinsky rotation between trans bend and symmetric stretch by about 5% and increases Duschinsky rotation between trans bend and C–C stretch by about 3%.

The use of curvilinear coordinates, on the other hand, appears to have a much more profound impact on the coordinate transformation. The rectilinear displacement vectors $\boldsymbol{\delta}^{(0)}$ and $\boldsymbol{\delta}^{(\text{a-s})}$ both exhibit a large displacement along the symmetric C—H stretch coordinate, q'_1, even though the equilibrium geometries of the $\tilde{A}$ and $\tilde{X}$ states have nearly identical C—H bond lengths (Figure 3). The use of curvilinear coordinates removes displacement along $\bar{q}'_1$ almost entirely. The reason for the displacement in the rectilinear stretching coordinate is that the rectilinear bending coordinate q'_3 stretches the C—H bond. The result is that in order to arrive at the linear $\tilde{X}$-state equilibrium from the trans-bent $\tilde{A}$-state equilibrium it is necessary to straighten the molecule by a negative displacement in q'_3 and then contract the elongated C—H bond by a negative displacement in q'_1. The small value of $\delta_1^{(\text{c-l})}$ is consistent with the experimental observation that there is very little Franck-Condon activity in ν'_1. Furthermore, the rectilinear coordinate transformations (Tables VI and VII) exhibit a large Duschinsky rotation between the bending and C—H stretch coordinates in both the a_g block ($D_{1',4b''}$) and the b_u block ($D_{5',5b''}$), whereas the use of the curvilinear harmonic basis decreases these off-diagonal elements of the Duschinsky matrix by almost two orders of magnitude.

IV. EVALUATION OF CALCULATED FC INTENSITIES FOR THE *GERADE* MODES

We first evaluate FC intensities for transitions involving only *gerade* vibrational modes. The results are compared with

TABLE VI. Elements of the zeroth order Duschinsky matrix $\mathbf{D}^{(0)}$ and displacement vector $\boldsymbol{\delta}^{(0)}$ for the $\tilde{A}$—$\tilde{X}$ transition of acetylene calculated by Eqs. (87) and (88) from the **l** matrices from Tables IV and V (using the force fields of Ref. 65 for the $\tilde{X}$ state and Ref. 64 for the $\tilde{A}$ state.)

	$\mathbf{D}^{(0)}$						
	q''_1	q''_2	q''_{4b}	q''_3	q''_{5b}	q''_{5c}	$\boldsymbol{\delta}^{(0)}$
q'_1	0.8081	0.0415	1.5628	0	0	0	−4.3103
q'_2	−0.1303	0.8490	0.0857	0	0	0	−2.1803
q'_3	−0.3764	−0.1134	0.9754	0	0	0	−6.2585
q'_5	0	0	0	0.6672	1.424	0	0
q'_6	0	0	0	−0.3428	0.7324	0	0
q'_4	0	0	0	0	0	1.0275	0

TABLE VII. Elements of the Duschinsky matrix $\mathbf{D}^{(\text{a-s})}$ and displacement vector $\boldsymbol{\delta}^{(\text{a-s})}$ for the $\tilde{A}$—$\tilde{X}$ transition of acetylene, with first-order corrections for axis switching, are calculated from equations Eqs. (26) and (27), evaluated using the **l** and $\mathbf{l}_{\mathbf{R}}$ matrices from Tables IV and V.

	$\mathbf{D}^{(\text{a-s})}$						
	q''_1	q''_2	q''_{4b}	q''_3	q''_{5b}	q''_{5c}	$\boldsymbol{\delta}^{(\text{a-s})}$
q'_1	0.7571	0.0718	1.4347	0	0	0	−3.931
q'_2	−0.1104	0.8396	0.1247	0	0	0	−2.257
q'_3	−0.3497	−0.1244	1.0154	0	0	0	−6.321
q'_5	0	0	0	0.6917	1.3700	0	0
q'_6	0	0	0	−0.3297	0.7593	0	0
q'_4	0	0	0	0	0	1.0275	0

TABLE VIII. Elements of the Duschinsky matrix $\mathbf{D}^{(c\text{-}l)}$ and displacement vector $\boldsymbol{\delta}^{(c\text{-}l)}$ for the $\tilde{A}$—$\tilde{X}$ transition of acetylene, performed in the basis of harmonic wavefunctions of curvilinear normal mode coordinates, are calculated from equations Eqs. (41) and (42), evaluated using the **l** matrices from Tables IV and V.

	$\mathbf{D}^{(c\text{-}l)}$						
	$\bar{q}_1''$	$\bar{q}_2''$	$\bar{q}_{4b}''$	$\bar{q}_3''$	$\bar{q}_{5b}''$	$\bar{q}_{5c}''$	$\boldsymbol{\delta}^{(c\text{-}l)}$
$\bar{q}_1'$	0.9215	0.1805	0.0144	0	0	0	0.1021
$\bar{q}_2'$	−0.0916	0.8404	−0.0893	0	0	0	−0.9681
$\bar{q}_3'$	−0.0084	0.0431	1.3240	0	0	0	−7.400
$\bar{q}_5'$	0	0	0	0.9427	−0.0733	0	0
$\bar{q}_6'$	0	0	0	0.0176	1.0350	0	0
$\bar{q}_4'$	0	0	0	0	0	1.0275	0

experiment and with the calculation by Watson.[46] Transitions involving *ungerade* modes will be considered in Paper II[72] of this series.

A. $v_3' \leftarrow 0$ progression

The most prominent feature in the ground state $\tilde{A} \leftarrow \tilde{X}$ absorption spectrum is the strong Franck-Condon progression in v_3'. Table IX and Figure 4 provide a comparison between experimental absorption data and calculated relative intensities using both the Tobiason *et al.*[66] force field and the Jiang *et al.*[64] force field, and using the three types of coordinate transformation discussed in Sec. III. The oscillator strengths in Table IX were calculated according to

$$f = \frac{4\pi m_e c \nu_{0\text{-}0}}{3\hbar e^2} |\langle \Psi_{el}' | \mu_c | \Psi_{el}'' \rangle|^2 |\langle \Psi_{vib}' | q_4'' | \Psi_{vib}'' \rangle|^2, \quad (89)$$

where $\nu_{0\text{-}0}$ is the transition frequency between the ground vibrational levels of the two electronic states (in wavenumber units), m_e and e are the electron mass and charge and c is the speed of light. The quantity $\langle \Psi_{el}' | \mu_c | \Psi_{el}'' \rangle$ was estimated by taking the value of the *ab initio* electronic transition dipole moment (plotted in Figure 1) at the geometry $\mathbf{q}_0''$ (defined in Eq. (78)) that maximizes the exponential factor in the vibrational overlap integral.

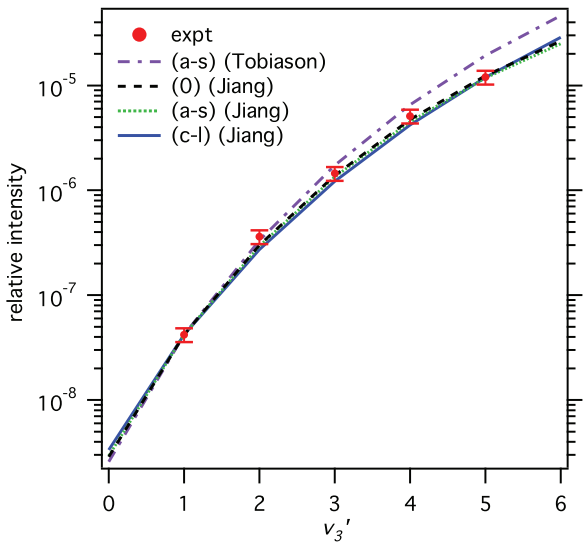

FIG. 4. The experimentally observed oscillator strengths from Ref. 2 for the $v_3' \leftarrow 0$ progression for the $\tilde{A} \leftarrow \tilde{X}$ system of acetylene are plotted with the reported error of 15% (red markers). Calculated vibrational intensity factors are shown for comparison. The calculated values were obtained using the Tobiason *et al.*[66] force field with the axis-switching transformation in Table VII (purple dash-dot curve); and the Jiang *et al.*[64] force field with the zero-order transformation of Table VI (black dashed curve), the axis-switching transformation of Table VII (green dotted curve), and the curvilinear transformation of Table VIII. The calculations are scaled to match the experimental f_{obs} for $v_3' = 1$.

Inspection of the trends in Table IX reveals that the calculations appear to underestimate the absolute magnitude of the vibrationless 0–0 transition by approximately three orders of magnitude. The Franck-Condon factor for the 0–0 transition is sensitively dependent on the displacement in equilibrium geometry between the two electronic states, and the equilibrium geometries are far from the geometry $\mathbf{q}_0$ that

TABLE IX. Observed oscillator strengths (f_{obs}) for the $v_3' \leftarrow 0$ progression of the $\tilde{A} \leftarrow \tilde{X}$ transition of acetylene and calculated vibrational intensity factors obtained using two different $\tilde{A}$-state force fields and three different types of coordinate transformation.

$\tilde{A}$-State FF:		Tobiason *et al.*[66]		Jiang *et al.*[64]					
Coord. trans.:		(a-s)[a]		(0)[b]		(a-s)[a]		(c-l)[c]	
v_3'	f_{obs}[d] $\times 10^8$	f_{calc} $\times 10^{12}$	f_{obs}/f_{calc} $\times 10^3$	f_{calc} $\times 10^{12}$	f_{obs}/f_{calc} $\times 10^3$	f_{calc} $\times 10^{12}$	f_{obs}/f_{calc} $\times 10^3$	f_{calc} $\times 10^{12}$	f_{obs}/f_{calc} $\times 10^3$
0		1.22		0.744		0.977		3.95	
1	4.2	19.9	2.11	10.9	3.86	14.0	3.01	49.4	0.849
2	36	158	2.28	77.6	4.64	97.9	3.68	321	1.12
3	145	819	1.77	360.	4.03	447	3.24	1430	1.01
4	510	3103	1.64	1220	4.18	1500	3.41	4930	1.03
5	1200	9170	1.31	3220	3.73	3910	3.07	13970	0.859
Mean:			1.82		4.09		3.28		0.976
SD:			21%		8.7%		8.3%		12%

[a]Calculated using the coordinate transformation in Eqs. (26) and (27).
[b]Calculated using the coordinate transformation in Eqs. (87) and (88).
[c]Calculated using the coordinate transformation in Eqs. (41) and (42).
[d]Values from Ref. 2. The measurement uncertainty is 15%.

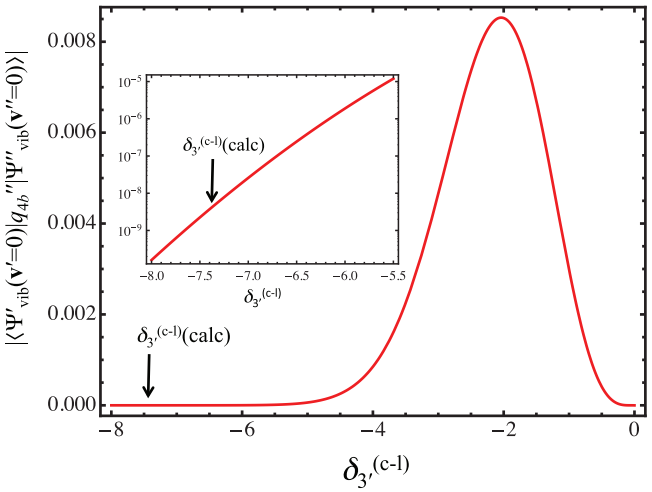

FIG. 5. The magnitude of the vibrational intensity factor $|\langle\Psi'_{vib}(\mathbf{v}'=0)|q''_{4b}|\Psi''_{vib}(\mathbf{v}''=0)\rangle|^2$ for the vibrationless 0–0 transition is shown as a function of the displacement in the trans-bending mode $\delta_{3'}$ between the equilibrium geometries of the $\tilde{A}$ and $\tilde{X}$ states of acetylene. All other parameters of the coordinate transformation are held fixed to the values in Table VIII. The arrow points to the calculated value of $\delta_{3'}^{(c\text{-}l)}$, and the inset displays a magnified region plotted on a logarithmic scale.

maximizes the exponential factor in the vibrational overlap integral. Using the curvilinear coordinate transformation in Table VIII, we find that $\mathbf{q_0}$ is located at a displacement of $(\bar{q}''_1, \bar{q}''_2, \bar{q}''_{4b}) = (-0.18, 0.68, 3.17)$. Because the $\tilde{A}$—$\tilde{X}$ transition intensity accumulates at geometries involving large-amplitude displacement in the trans-bending coordinate, q'_3, the failure of the calculation to match the experimentally observed oscillator strength is likely due to the fact that the large-amplitude q'_3 displacement is not well described in the harmonic basis. The use of curvilinear normal mode coordinates mitigates the discrepancy, but only by a factor of ∼3–4. In Figure 5, the vibrational intensity factor for the 0–0 transition is plotted as a function of $\delta_{3'}^{(c\text{-}l)}$ with all other parameters held fixed to the values in Table VIII. The intensity increases rapidly as the magnitude of $\delta_{3'}^{(c\text{-}l)}$ decreases. A change in $\delta_{3'}^{(c\text{-}l)}$ by ∼20% would give rise to a factor of $\sim 10^3$ increase in intensity. Including higher-order corrections for the anharmonicity in the trans-bending mode may help to bring the calculation into better agreement with experiment, but that is beyond the scope of the current work.

Although the absolute oscillator strength of the 0–0 transition is underestimated, the trend in the scaled vibrational intensities for the $v'_3 \leftarrow 0$ progression (shown in Figure 4) is in good agreement with experiment. The Franck-Condon factors obtained using the Tobiason *et al.* force field match Watson's calculation, which used the same force field and coordinate transformation. These intensities increase slightly too rapidly with v'_3. The trend in intensities calculated with the Jiang *et al.* force field seems to provide excellent agreement with experiment, such that it is difficult to distinguish the traces on the scale plotted in Figure 4. Throughout the rest of this series of papers, we will use the more recent Jiang force field.

B. Emission from $\tilde{A}(2^j3^k)$

Quantitative experimental intensity data are also available from dispersed fluorescence measurements in the dominant intensity Franck-Condon progressions ($2^j_m V^k_n$), where V refers to quanta in the trans-bending mode v'_3 or v''_4.[71] Trends in emission intensities from the $\tilde{A}$-state origin, 3^2, 2^13^1, and 2^13^2 levels are shown in Figure 6, and the calculated intensities obtained from the coordinate transformations in Tables VI–VIII are shown for comparison. The dispersed fluorescence spectra from Ref. 71 were recorded on a CCD (charge-coupled device) detector attached to a monochromator, and the relative intensities in each emission spectrum were calibrated by dispersing a halogen lamp to the same detector. Therefore, the relative intensities within each spectrum are well determined. However, due to variation and fluctuation in the intensity of the laser power used to excite each spectrum, the relative intensities between spectra from different $\tilde{A}$-state vibrational levels was not determined. As a result, the reported intensities in Ref. 71 are normalized relative to the strongest transition in each spectrum. For comparison, the calculated intensities shown in Figure 6 are normalized in the same way, by setting the strongest calculated vibronic intensity in each emission spectrum equal to one.

It is evident in Figure 6 that the effects of using curvilinear normal mode coordinates are much more profound than the effects of correcting for axis switching. In fact, the emission intensities obtained from the axis-switching coordinate transformation (Table VII) are so close in magnitude to those obtained from the zero-order coordinate transformation (Table VI) that it is difficult to tell the traces apart in some of the panels of the figure. The various calculations do a comparable job at reproducing the emission trends along v''_2. The zero-order transformation and the axis-switching transformation correctly locate the node in emission from 2^13^1 and 2^13^2 at $v''_2 = 2$, whereas the curvilinear transformation places the node at $v''_2 = 1$. All three calculations underestimate the intensity of the second lobe relative to the first (probably as a result of anharmonicity), but the curvilinear transformation performs slightly better at predicting the shape of the overall intensity envelope along v''_2 progressions.

As one would expect, the curvilinear coordinate transformation notably improves the performance of the calculation at high quanta in the bending mode, v''_4. The rectilinear calculations fail to reproduce the emission intensity into v''_4 above ∼12 quanta of excitation. The reason for this is that the rectilinear coordinate transformations overestimate the Duschinsky rotation between q'_1 and q''_{4b} (see Tables VI and VII) due to the bend-stretch coupling induced by the coordinate system (as illustrated in Figure 2). On the other hand, the curvilinear calculation produces near-quantitative results up to 22 quanta of bend excitation. This is a remarkable result, given that this amount of bending energy is almost enough to reach the acetylene↔vinylindene reaction barrier at ∼15200 cm^{-1}. The experimentally observed Franck-Condon factors reported in Ref. 71 are based on a polyad fit model that takes into account fractionation of intensity within the pure-bending polyads with conserved quantum number $N_B = v''_4 + v''_5$. Therefore, most of the important resonance

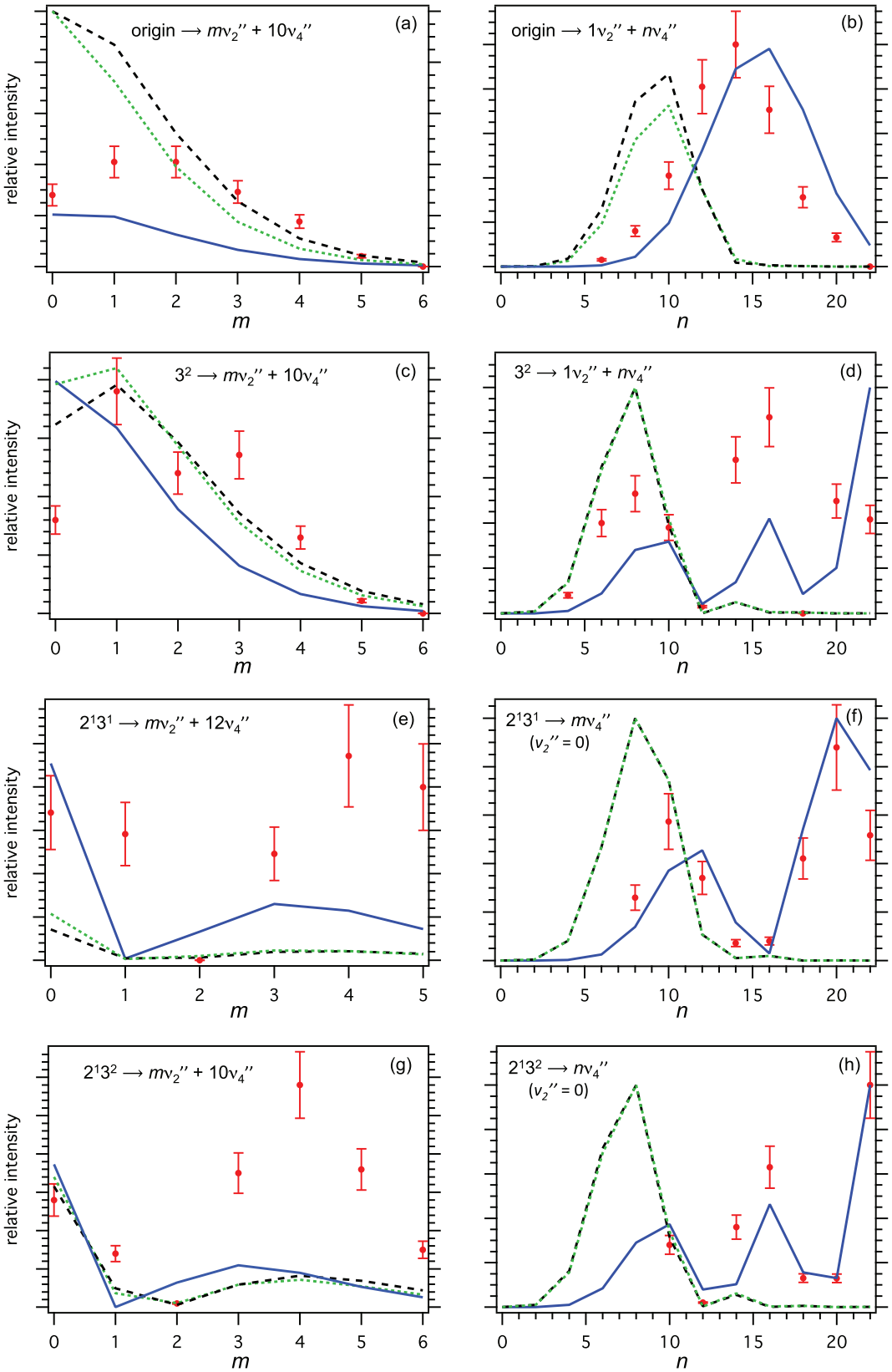

FIG. 6. Relative emission intensities for a selection of $(2^j_m V^k_n)$ vibrational transitions of the acetylene $\tilde{A} \rightarrow \tilde{X}$ transition. Emission is shown from the $\tilde{A}$ origin (panels (a) and (b)); 3^2 (panels (c) and (d)); $2^1 3^1$ (panels (e) and (f)); and $2^1 3^2$ (panels (g) and (h)). The left column of panels displays progressions in v_2'' (v_4'' held constant), and the right column of panels displays progressions in v_4'' (v_2'' held constant). The choice of which progression to plot was based on the availability of the most complete set of experimental data for comparison. Experimental intensities from dispersed fluorescence measurements were taken from Ref. 71 and are displayed as points with 15% uncertainty. The calculated intensities shown are the sum of the squares of vibrational overlap intensities to $|l_4''| = 0$ and $|l_4''| = 2$, obtained using the zero-order coordinate transformation in Table VI (dashed black curves), the axis-switching coordinate transformation in Table VII (green dotted curves), and the curvilinear coordinate transformation in Table VIII (blue solid curves). The observed and calculated intensities in the emission spectrum from each $\tilde{A}$-state vibrational level are normalized relative to the strongest vibronic transition in the spectrum.

interactions are already taken into account by the experiment, and the observed intensities represent the vibrational intensity into the *zero-order* bright state, which has all of the excitation in the trans-bend. Because the pure-bending polyad quantum number is known to be approximately conserved up to at least 22 quanta of bend excitation,[27] it is therefore not too surprising that a harmonic calculation—performed in the correct basis—reproduces the experimentally observed intensity pattern.

V. CONCLUSIONS

There are obvious limitations to treating FC factors of the $\tilde{A}$—$\tilde{X}$ system of acetylene in the harmonic basis, and we do not expect complete quantitative agreement with experimental intensities. Because of the large displacement in equilibrium geometry between the two states, the harmonic calculation is unable to reproduce the observed oscillator strength for the vibrationless 0–0 transition. However, we have shown that a simple computational method can effectively reproduce qualitative trends in the spectrum.

We have shown how the methods developed by Watson[46,48,61] for calculating Franck-Condon factors for electronic transitions involving linear↔nonlinear geometry changes may be generalized to full dimensionality. The methods outlined in this paper may also be applied to any linear↔nonlinear transition, provided that most of the value of the integral does not accumulate at the linear geometry, where the $n_{\text{vib}} = 3N - 6$ treatment becomes invalid. One of the components of a degenerate bending mode may always be chosen to correlate with a-axis rotation in the nonlinear state. The angular component of this mode may be constrained and its $\mathbf{l}$ vector may then be moved into $\mathbf{l}_{\mathbf{R}}$. To simplify the integration of the generating function, the remaining degenerate bending modes may be treated in the Cartesian two-dimensional harmonic oscillator basis, and the resulting integral will have a form similar to Eq. (70). The basis set conversion to (v, l) quantum numbers that describe the two-dimensional harmonic oscillators in polar coordinates may be performed after the overlap integrals have been calculated.

Furthermore, in π-bonded systems it is very common to have large-amplitude bending displacements between the equilibrium geometries of different electronic states. The reason is that an electronic $\pi^* \leftarrow \pi$ excitation effectively changes the sp^n hybridization, which leads to a qualitative change in equilibrium bond angle. As a result, such electronic transitions are accompanied by long Franck-Condon progressions in modes involving the displaced bending coordinates. As demonstrated in this paper, simple methods for working in curvilinear normal mode coordinates are capable of producing notable improvement the intensity progressions at high quanta of bend excitation that occur in these cases.

Finally, our FC calculations have provided a test of the new force field for $\tilde{A}$-state acetylene reported by Jiang *et al.*[64] The force field takes into account new data that were not previously available. The new force field appears to produce improved agreement with experiment along the dominant intensity FC progressions.

ACKNOWLEDGMENTS

The author is grateful to Robert W. Field for providing guidance and mentorship on this work. The author would also like to thank James K. G. Watson, Joshua H. Baraban, P. Bryan Changala, and Jun Jiang for helpful discussions. This material is based on work supported by the U.S. Department of Energy, Office of Science, Chemical Sciences, Geosciences and Biosciences Division of the Basic Energy Sciences Office, under Award Number DE-FG0287ER13671.

[1] G. W. King and C. K. Ingold, Nature (London) **169**(4313), 1101–1102 (1952).
[2] C. K. Ingold and G. W. King, J. Chem. Soc. **1953**, 2702–2755 (1953).
[3] K. K. Innes, J. Chem. Phys. **22**(5), 863–876 (1954).
[4] E. K. Plyler, E. D. Tidwell, and T. A. Wiggins, J. Opt. Soc. Am. **53**, 589–593 (1963).
[5] J. Plíva, J. Mol. Spectrosc. **44**(1), 145–164 (1972).
[6] K. F. Palmer, M. E. Mickelson, and K. N. Rao, J. Mol. Spectrosc. **44**(1), 131–144 (1972).
[7] A. Baldacci, S. Ghersetti, and K. N. Rao, J. Mol. Spectrosc. **68**(2), 183–194 (1977).
[8] A. Baldacci, S. Ghersetti, and K. N. Rao, J. Mol. Spectrosc. **41**(1), 222–225 (1972).
[9] L. Sinitsa, J. Mol. Spectrosc. **84**(1), 57–59 (1980).
[10] B. C. Smith and J. S. Winn, J. Chem. Phys. **89**(8), 4638–4645 (1988).
[11] J. K. G. Watson, M. Herman, J. C. V. Craen, and R. Colin, J. Mol. Spectrosc. **95**(1), 101–132 (1982).
[12] J. C. V. Craen, M. Herman, R. Colin, and J. K. G. Watson, J. Mol. Spectrosc. **111**(1), 185–197 (1985).
[13] J. C. V. Craen, M. Herman, R. Colin, and J. K. G. Watson, J. Mol. Spectrosc. **119**(1), 137–143 (1986).
[14] M. Herman, T. Huet, and M. Vervloet, Mol. Phys. **66**(2), 333–353 (1989).
[15] W. Lafferty and A. Pine, J. Mol. Spectrosc. **141**(2), 223–230 (1990).
[16] R. D'Cunha, Y. Sarma, G. Guelachvili, R. Farrenq, Q. Kou, V. Devi, D. Benner, and K. N. Rao, J. Mol. Spectrosc. **148**(1), 213–225 (1991).
[17] A.-M. Tolonen and S. Alanko, Mol. Phys. **75**(5), 1155–1165 (1992).
[18] Y. Kabbadj, M. Herman, G. D. Lonardo, L. Fusina, and J. Johns, J. Mol. Spectrosc. **150**(2), 535–565 (1991).
[19] J. Vanderauwera, D. Hurtmans, M. Carleer, and M. Herman, J. Mol. Spectrosc. **157**(2), 337–357 (1993).
[20] Q. Kou, G. Guelachvili, M. A. Temsamani, and M. Herman, Can. J. Phys. **72**(11-12), 1241–1250 (1994).
[21] M. A. Temsamani and M. Herman, J. Chem. Phys. **102**(16), 6371–6384 (1995).
[22] S. A. B. Solina, J. P. O'Brien, R. W. Field, and W. F. Polik, J. Phys. Chem. **100**(19), 7797–7809 (1996).
[23] M. A. Temsamani, M. Herman, S. A. B. Solina, J. P. O'Brien, and R. W. Field, J. Chem. Phys. **105**(24), 11357–11359 (1996).
[24] M. P. Jacobson, J. P. O'Brien, R. J. Silbey, and R. W. Field, J. Chem. Phys. **109**(1), 121–133 (1998).
[25] M. P. Jacobson, C. Jung, H. S. Taylor, and R. W. Field, J. Chem. Phys. **111**(2), 600–618 (1999).
[26] M. I. El Idrissi, J. Liévin, A. Campargue, and M. Herman, J. Chem. Phys. **110**(4), 2074–2086 (1999).
[27] M. P. Jacobson and R. W. Field, J. Phys. Chem. A **104**(14), 3073–3086 (2000).
[28] K. Hoshina, A. Iwasaki, K. Yamanouchi, M. P. Jacobson, and R. W. Field, J. Chem. Phys. **114**(17), 7424–7442 (2001).
[29] M. Herman, A. Campargue, M. I. E. Idrissi, and J. V. Auwera, J. Phys. Chem. Ref. Data **32**(3), 921–1361 (2003).
[30] J. D. Tobiason, A. L. Utz, and F. F. Crim, J. Chem. Phys. **99**(2), 928–936 (1993).
[31] A. L. Utz, J. D. Tobiason, E. Carrasquillo M, L. J. Sanders, and F. F. Crim, J. Chem. Phys. **98**(4), 2742–2753 (1993).
[32] M. Mizoguchi, N. Yamakita, S. Tsuchiya, A. Iwasaki, K. Hoshina, and K. Yamanouchi, J. Phys. Chem. A **104**(45), 10212–10219 (2000).
[33] A. J. Merer, N. Yamakita, S. Tsuchiya, J. F. Stanton, Z. Duan, and R. W. Field, Mol. Phys. **101**(4–5), 663–673 (2003).
[34] A. H. Steeves, A. J. Merer, H. A. Bechtel, A. R. Beck, and R. W. Field, Mol. Phys. **106**(15), 1867–1877 (2008).

[35]A. J. Merer, N. Yamakita, S. Tsuchiya, A. H. Steeves, H. A. Bechtel, and R. W. Field, J. Chem. Phys. **129**(5), 054304 (2008).
[36]A. H. Steeves, H. A. Bechtel, A. J. Merer, N. Yamakita, S. Tsuchiya, and R. W. Field, J. Mol. Spectrosc. **256**(2), 256–278 (2009).
[37]A. J. Merer, A. H. Steeves, J. H. Baraban, H. A. Bechtel, and R. W. Field, J. Chem. Phys. **134**(24), 244310 (2011).
[38]F. Duschinsky, Acta Physicochim. URSS **7**, 551–556 (1937).
[39]B. A. Mamedov, H. Koc, and N. Sunel, J. Mol. Struct. **1048**, 301–307 (2013).
[40]T. E. Sharp and H. M. Rosenstock, J. Chem. Phys. **41**(11), 3453–3463 (1964).
[41]W. L. Smith and P. A. Warsop, Trans. Faraday Soc. **64**, 1165–1173 (1968).
[42]M. A. Kovner, A. V. Gorokhov, G. A. Gerasimov, and E. N. Bazarov, Opt. Spectrosc. **29**(4), 356–359 (1970).
[43]T. Müller, P. Dupre, P. Vaccaro, F. Pérez-Bernal, M. Ibrahim, and F. Iachello, Chem. Phys. Lett. **292**(3), 243–253 (1998).
[44]H. Ishikawa, H. Toyosaki, N. Mikami, F. Pérez-Bernal, P. Vaccaro, and F. Iachello, Chem. Phys. Lett. **365**(1–2), 57–68 (2002).
[45]I. Kanesaka and K. Kawai, Bull. Chem. Soc. Jpn. **48**(10), 2745–2750 (1975).
[46]J. K. G. Watson, J. Mol. Spectrosc. **207**(2), 276–284 (2001).
[47]J. Weber and G. Hohlneicher, Mol. Phys. **101**(13), 2125–2144 (2003).
[48]J. T. Hougen and J. K. G. Watson, Can. J. Phys. **43**, 298–320 (1965).
[49]J. H. Baraban, A. R. Beck, A. H. Steeves, J. F. Stanton, and R. W. Field, J. Chem. Phys. **134**(24), 244311 (2011).
[50]J. H. Baraban, Personal communication (2014).
[51]D. M. Jonas, S. A. B. Solina, B. Rajaram, R. J. Silbey, R. W. Field, K. Yamanouchi, and S. Tsuchiya, J. Chem. Phys. **97**(4), 2813–2816 (1992).
[52]İ. Özkan, J. Mol. Spectrosc. **139**(1), 147–162 (1990).
[53]E. B. Wilson, J. C. Decius, and P. C. Cross, *Molecular Vibrations: The Theory of Infrared and Raman Vibrational Spectra* (McGraw-Hill, New York, 1955).
[54]A. R. Hoy, I. M. Mills, and G. Strey, Mol. Phys. **24**(6), 1265 (1972).
[55]R. Borrelli and A. Peluso, J. Chem. Phys. **125**(19), 194308 (2006).
[56]R. Borrelli and A. Peluso, J. Chem. Phys. **139**(15), 159902 (2013).
[57]J. R. Reimers, J. Chem. Phys. **115**(20), 9103–9109 (2001).
[58]A. Capobianco, R. Borrelli, C. Noce, and A. Peluso, Theor. Chem. Acc. **131**(3), 1181 (2012).
[59]R. Borrelli, A. Capobianco, and A. Peluso, Can. J. Chem. **91**(7), 495–504 (2013).
[60]R. Botter, V. H. Dibeler, J. A. Walker, and H. M. Rosenstock, J. Chem. Phys. **44**, 1271–1278 (1966).
[61]J. K. G. Watson, Mol. Phys. **79**(5), 943–951 (1993).
[62]D. M. Jonas, X. Yang, and A. M. Wodtke, J. Chem. Phys. **97**(4), 2284–2298 (1992).
[63]C. Cohen-Tannoudji, B. Diu, and F. Laloë, *Quantum Mechanics* (Hermann, Paris, 1977).
[64]J. Jiang, J. H. Baraban, G. B. Park, M. L. Clark, and R. W. Field, J. Phys. Chem. A **117**(50), 13696–13703 (2013).
[65]L. Halonen, M. S. Child, and S. Carter, Mol. Phys. **47**(5), 1097–1112 (1982).
[66]J. D. Tobiason, A. L. Utz, E. L. Sibert, and F. F. Crim, J. Chem. Phys. **99**(8), 5762–5767 (1993).
[67]M. P. Jacobson, J. P. O'Brien, and R. W. Field, J. Chem. Phys. **109**(10), 3831–3840 (1998).
[68]J. H. Baraban, P. B. Changala, A. J. Merer, A. H. Steeves, H. A. Bechtel, and R. W. Field, Mol. Phys. **110**(21–22), 2707–2723 (2012).
[69]J. H. Baraban, A. J. Merer, J. F. Stanton, and R. W. Field, Mol. Phys. **110**(21-22), 2725–2733 (2012).
[70]J. H. Baraban, personal communication (2014).
[71]J. P. O'Brien, "Acetylene: Dispersed fluorescence spectroscopy and intramolecular dynamics," Ph.D. thesis (Massachusetts Institute of Technology, 1991).
[72]G. B. Park, J. H. Baraban, and R. W. Field, "Full dimensional Franck–Condon factors for the acetylene $\tilde{\mathbf{A}}^{\mathbf{1}}\mathbf{A}_{\mathbf{u}}$—$\tilde{\mathbf{X}}^{\mathbf{1}}\Sigma_{\mathbf{g}}^{+}$ transition. II. Vibrational overlap factors for levels involving excitation in *ungerade* modes," J. Chem. Phys. **141**, 134305 (2014).